Coordination Chemistry Reviews 255 (2011) 2469–2502

Contents lists available at ScienceDirect

Coordination Chemistry Reviews

journal homepage: www.elsevier.com/locate/ccr

Review

Metal-containing polymers: Facile tuning of photophysical traits and emerging applications in organic electronics and photonics

Cheuk-Lam Ho, Wai-Yeung Wong*

Institute of Molecular Functional Materials,[1] Department of Chemistry and Centre for Advanced Luminescence Materials, Hong Kong Baptist University, Waterloo Road, Kowloon Tong, Hong Kong, PR China

Contents

Abbreviations: acac, acetylacetonate; Alq$_3$, tris(8-hydroxyquinolinato)aluminum; bpy, 2,2′-bipyridine; bpym, 5,5′-bipyrimidine; CIE, Commission International de L'Eclairage; CT, charge-transfer; Da, Dalton unit; D–A, donor–acceptor; dfppy, 2-(2,4-difluorophenyl)pyridine; DMF, dimethylformamide; E_g, optical bandgap; EL, electroluminescence; EQE, external quantum efficiency; FF, fill factor; HOMO, highest occupied molecular orbital; ICT, intramolecular charge transfer; IL, intraligand; IPCE, incident photon-to-electron conversion efficiency; J_{sc}, short-circuit current; LC, ligand-centered; LE, luminance efficiency; LED, light-emitting diode; LUMO, lowest unoccupied molecular orbital; MLCT, metal-to-ligand charge transfer; MW, molecular weight; NIR, near-infrared; OFET, organic field-effect transistor; PCBM, [6,6]-phenyl-C$_{61}$-butyric acid methyl ester; PCE, power conversion efficiency; PE, power efficiency; PEDOT:PSS, poly(ethylenedioxythiophene)–poly(styrenesulfonic acid); PFB, poly(9,9-dioctylfluorene-co-bis-*N*,*N*-(4-butylphenyl)-bis-*N*,*N*-phenyl-1,4-phenylenediamine); PHOLED, phosphorescent organic light-emitting diode; PL, photoluminescence; PLED, polymer light-emitting diode; PPV, poly(*p*-phenylene vinylene)s; ppy, 2-phenylpyridine; pq, 2-phenylquinoline; PVK, poly(*N*-vinylcarbazole); S_1, first singlet excited state; salen, *N*,*N*′-ethylenebis(salicylimine); SCLC, space charge limited current; salen, *N*,*N*′-ethylenebis(salicylimine); T_1, first triplet excited state; terpy, 2,2′:6′,2″-terpyridine; tpys, 2-*p*-tolylpyrazole; tpzs, 1-*p*-tolylpyrazole; UV–vis, ultraviolet–visible; WPLED, white polymer light-emitting diode; Φ_{PL}, photoluminescence quantum yield; λ_{max}, absorption wavelength maximum; λ_{em}, emission wavelength; μ_h, hole mobility; μ_e, electron mobility.

* Corresponding author. Tel.: +852 34117074; fax: +852 34117348.
E-mail address: rwywong@hkbu.edu.hk (W.-Y. Wong).

[1] Areas of Excellence Scheme, University Grants Committee (Hong Kong).

0010-8545/$ – see front matter
doi:10.1016/j.ccr.2011.01.052

ARTICLE INFO

Article history:
Received 16 October 2010
Accepted 25 January 2011
Available online 8 February 2011

Keywords:
Metallopolymers
Photoluminescence
Photophysics
Organic electronics
Transition metals

ABSTRACT

Metal-containing polymers or metallopolymers have become a field of immense interest because of their possible application in the materials industry. The presence of transition metal elements in a polymer chain would offer an attractive platform for combining the chemical, electronic, magnetic, optical and redox properties of metal complexes with those of the organic materials. This has led to a rapidly expanding knowledge in their functional properties and uses. A complete understanding of the relationship between chemical and electronic structures is necessary to tailor for a particular function so that specialty polymers with advanced functionalities can be developed. Polymers possess unique advantages such as low cost, light weight and ease of solution processibility and, therefore, they hold great promise as versatile functional materials for exploitation in organic electronics. This review presents the latest research development of the field, with emphasis on fundamental concepts, facile tuning of their photophysical properties and current applications in the optoelectronic areas. To date, many soluble, semiconducting, photovoltaic and luminescent conjugated metalated polymers have been generated and studied. They have found an array of high-tech applications, for example, as active layers in the fabrication of polymer light-emitting diodes, polymer solar cells and polymer field-effect transistors. Their excited state chemistry is also of pivotal importance in understanding the operation mechanism and in optimizing the performance of these polymeric optoelectronic devices. This contribution will serve as a good forum to highlight the contemporary developments made by the polymer scientists working on functional metal-containing polymers for organic electronics and photonics.

1. Introduction

Nowadays, new functional materials with tailor-made properties, low-temperature solution-processing features with less waste of materials, low cost and straightforward synthesis are of central importance in the themes of material sciences especially in large area applications such as lighting [1] and light harvesting [2,3]. Polymer materials have rapidly found wide applications as construction materials, chiefly owing to those properties including their resistance to corrosion, low specific gravity, aesthetic appearance, etc. that make them superior to metals or inorganic matrices [4]. However, polymer materials also have disadvantages that are not shared by metals. Compared to metals, they have lower mechanical strength and relatively low thermal stability. Hence, the idea of combining polymers and metals into metallopolymers that exhibit as many advantages of either parent material as possible but with the number of their disadvantages reduced to a minimum has significant appeal. In this way, materials with properties typical of insulators, semiconductors, and even conductors, can be obtained. Introduction of transition metal ions into π-conjugated polymers provides the opportunity to further tune the physical properties of the resulting metal–organic hybrid materials [5–9]. Therefore, the strong interaction between organic and inorganic components creates unique photophysical, electrochemical and photochemical properties, which make these conjugated polymers potential materials for applications in electroluminescence, solar energy conversion, sensors, nonlinear optics and photo-refraction [10–13].

In metallopolymers, metal atoms form an integral part of the main chain or side group structure of a polymer. Besides physical properties, the photoluminescence (PL) properties of these metalated polymers are also affected by the metal and polymer interactions. By varying the structure of the ligand and/or the metal complex, it is possible to fine-tune the electronic properties of the resulting metallopolymers. Several features that are unique to metal–organic systems include the strong electronic interaction between the transition metal and π-delocalized electron system and the rich chemistry of transition metal complexes and conjugated polymers [14–19]. The property investigations have not only shed light on the structure–property relationships but also led to the development of specialty polymers with advanced functionalities [20–29]. Due to the versatile properties of metal–organic hybrid materials, there is significant promise that these materials can play key roles in polymer light-emitting diodes (PLEDs) and solar cells.

The harvesting of energy from the triplet states is an increasingly important goal in research on organic-based light-emitting diodes (LEDs), because electrophosphorescent devices utilizing emission from triplet states (i.e. phosphorescence) have potentially much higher efficiencies than those emission only from singlet states [30,31]. Since phosphorescence from conjugated organic polymers, if present, is generally very weak, the wasted triplet energy can be harnessed by the incorporation of heavy metal complexes into the polymers. Moreover, in metallopolymers, both the conjugated organic backbone and the metal complex can each emit light upon excitation by photons and electrons. As a result, it is possible to tune the emission color in PLEDs by choosing different monomers or changing the loading amount of metal complex to the polymer. On the other hand, photovoltaic cells act in the opposite way to LEDs in that light is absorbed for electricity generation. Materials having a delocalized π-electron system can absorb sunlight, create photogenerated charge carriers and transport them. To fully exploit the endless source of solar energy, the absorption spectrum of a conjugated polymer needs to cover both the red and near-infrared (NIR) ranges to match the greater part of the terrestrial solar spectrum and hence harvest the maximum photon flux. It is highly desirable to develop conjugated polymers with broader absorptions through narrowing their optical bandgap (E_g). The absorption of polymers can be extended to the NIR easily by incorporation of appropriate metal complexes. Furthermore, to efficiently absorb light, it is necessary to have high overall extinction coefficients of the polymers which should not be sacrificed as the E_g becomes smaller. Metallopolymers can give high absorptivities especially in the low-energy region. Therefore, metallopolymers become more important in the field of photovoltaic cells, especially for the ruthenium- and platinum-containing polymers.

In this review, we highlight the types and photophysics of various metal-containing polymeric systems, with special emphasis placed on those with zinc, ruthenium, iridium and platinum units. For these metallopolymers, their light-emitting and -absorbing properties are easily predictable and rationalized based on structural variations. We believe that the insight gained from

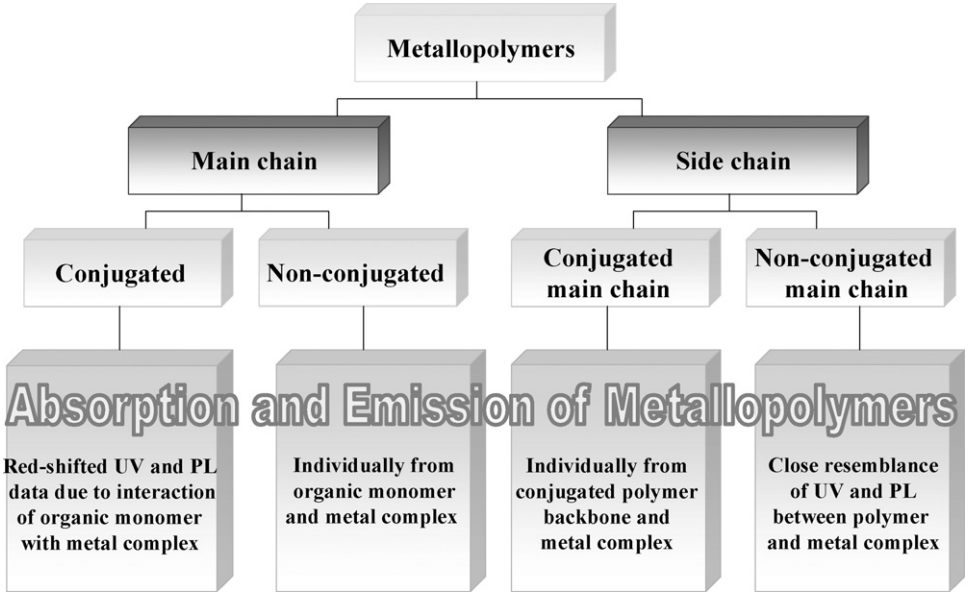

Fig. 1. Different categories of metallopolymers and their features.

these fundamental studies of the photophysics of π-conjugated metal–organic systems would provide useful guidelines for their use as active materials in optical and electronic devices and to address the special application needs.

2. Strategies for engineering the photoluminescence properties of metallopolymers

In general, there are two main types of metallopolymer, viz. metal complexes in the main chain or in a side chain. Various ways of tuning the photophysical properties of metallopolymers are summarized in Fig. 1. In the main-chain polymer, the metal complex core is embedded as a part of the polymer backbone. With the polymer fragment and metal chromophore attached by single, double or triple bonds, the polymer is fully conjugated and the metal center can interact with the polymer chain so that the photophysical properties are an amalgamation of both parts, usually resulting in a significant red-shifted absorption and emission spectra. If the monomer and metal complex are connected by amide, imine or ester group, the polymer backbone becomes non-conjugated. Their UV and PL spectra are mostly the sum-up from organic monomers and metal complexes individually. On the other hand, if the metal complexes are attached at the periphery of the conjugated polymers by alkyl chain, the polymer backbone and metal complex would absorb and emit light separately. Identical absorption and emission traits of the metallopolymers to the corresponding metal complex would appear if they were bonded to a non-conjugated polymer chain, for example, in the vinyl-type polymers. In each case, the content of metal unit in the polymer would greatly affect its photophysical properties.

3. Zinc-containing polymers

Zinc complexes and polymers have found numerous applications due to the high availability, low toxicity and low cost of zinc(II) ions and hence they show a considerable advantage compared with the other relevant metals [32]. A variety of systems containing Zn(II) ion with high PL quantum yields (Φ_{PL}) and electroluminescence (EL) performance have recently been synthesized. Their photophysical data are summarized in Table 1.

3.1. Zinc(II) Schiff base-containing polymers

Zinc(II) complexes with Schiff base ligands are promising materials for optoelectronic applications. The zinc(II)-salen type chromophore (salen = *N*,*N*′-ethylenebis(salicylimine)) was chosen as the architectural unit because the bis(*N*-alkylsalicylaldiminato) Zn(II) complex has excellent fluorescent properties with outstanding PL and EL properties, high Φ_{PL} and good thermal stability. The ease of synthesis allows structural modification for optimization of their material properties, and could be used as a fluorescent indicator and probe [33]. Che et al. first reported the preparation and applications of soluble self-assembled Zn(II) Schiff base polymers (**Zn-1**), which are thermally stable, structurally diverse and easily modified [34]. The polymers exhibit similar absorption patterns in dimethylformamide (DMF) with λ_{max} at 280–309 and 311–358 nm, which are assigned to the ligand-centered (LC) π–π* transitions of the *p*-phenyl rings and salicylaldimine ligands, in addition to a shoulder ranging from 408 to 427 nm. Their PL emissions are assigned to the intra-ligand $^1(\pi-\pi^*)$ fluorescence and span from blue to yellow in DMF solution (e.g. blue for **Zn-1b**, green for **Zn-1a** and **Zn-1c**, and yellow for **Zn-1h** with λ_{em} at 458, 508, 501, and 562 nm, respectively, upon photoexcitation at 360 nm). The Φ_{PL} ranges from 2% for **Zn-1e** and **Zn-1h** to 34% for **Zn-1f**. On the other hand, the films of most of these polymers emit yellowish-orange color with PL λ_{em} at 534–538 nm, except for **Zn-1b** (λ_{em} = 509 nm) and **Zn-1c** (λ_{em} = 526 nm). The emission from the film of **Zn-1g** (λ_{em} = 534 nm) shows a Stokes shift of approximately 870 cm^{-1}, attributed to the aromatic stacking excimer formation in the solid state. Polymer **Zn-1c** exhibits a more greenish emission compared to the other polymers, probably due to the presence of the bulky *t*-butyl groups which suppress the aggregation of the polymer chains and reduce the chance of excimer formation. Thus, the emission color can be fine-tuned easily by incorporation of different functional group R. Different EL spectra and device properties were also recorded as the R group alters. For instance, device with **Zn-1c** shows a green emission at 536 nm with CIE coordinates of (0.30, 0.55) at a bias voltage of 8 V. The maximum luminance efficiency (LE) of the device was 2.0 cd A^{-1} and the maximum luminance of 3120 cd m^{-2} was obtained at 15 V. While the device fabricated with **Zn-1g** exhibited an orange EL at 584 nm with CIE coordinates of (0.54, 0.45) at 6 V, its maximum LE was 2.6 cd A^{-1} at 8 V with the

Table 1
Photophysical data of Zn(II) metallopolymers.

Polymer	$\lambda_{max,abs}$[a] [nm]	$\lambda_{em,PL(sol)}$[b] [nm]	$\lambda_{em,PL(film)}$[c] [nm]	HOMO/LUMO[d] [eV]	E_g [eV]	Ref.
Zn-1a	315 (34.6), 351 (23.1), 408 (12.0)	508 (0.06)	538 (0.13)			[34]
Zn-1b	282 (20.7), 325 (28.7), 378 (11.0)	458 (0.09)	509 (0.04)			[34]
Zn-1c	291 (24.3), 311 (26.5), 413 (18.1)	501 (0.15)	536 (0.13)			[34]
Zn-1d	304 (27.2), 319 (26.0), 351 (30.1)	534 (<0.01)				[34]
Zn-1e	286 (57.7), 352 (24.1), 425 (11.4)	518 (0.02)	534 (0.07)			[34]
Zn-1f	305 (54.3), 322 (47.4), 345 (41.2)	516 (0.34)	538 (0.15)			[34]
Zn-1g	284 (34.6), 309 (32.3), 324 (30.1), 352 (26.0), 427 (3.5)	514 (0.20)	538 (0.19)			[34]
Zn-1h	280 (44.6), 358 (48.3)	562 (<0.01)				[34]
Zn-2a	358		531 (0.51)	6.14/3.23	2.89	[35]
Zn-2b	317, 379		540 (0.46)	6.13/3.21	2.84	[35]
Zn-2c	327, 372		546 (0.42)	6.15/3.20	2.85	[35]
Zn-3a	287, 328, 342	450 (0.45)	450 (0.20)	–/3.25	3.19	[38]
Zn-3b	290, 320, 343	439 (0.25)	436, 489 (0.30)	–/3.10	3.26	[38]
Zn-3c	287, 328, 345	457 (0.50)	465 (0.40)	–/3.10	3.20	[38]
Zn-3d	288, 326, 344	441 (0.44)	430 (0.25)	–/3.11	3.26	[38]
Zn-3e	287, 328, 342	422 (0.25)	488 (0.15)			[38]
Zn-3f	289, 328, 346, 373	457 (0.77)	546 (0.50)	–/3.20	2.95	[38]
Zn-3g	288, 346, 372	456 (0.34)	530 (0.20)	–/3.20	2.92	[38]
Zn-3h	287, 328, 342	434, 518 (0.32)	535 (0.55)	–/3.22	2.92	[38]
Zn-3i	286, 327, 391, 413	440, 461, 556 (0.49)	567 (0.40)	–/3.19	2.64	[38]
Zn-3j	288, 324, 414	459, 488[e] (0.15)		–/3.40	2.60	[32]
Zn-3k	286, 313, 405	501 (0.33)		–/3.50	2.48	[32]
Zn-3l	286, 326, 373	443 (0.23)		–/3.50	2.54	[32]
Zn-3m	286, 327, 403	468 (0.52)		–/3.54	2.63	[32]
Zn-3n	434, 438	477 (0.42)		–/3.51	2.41	[32]
Zn-3o	286, 331, 403	470, 496[e] (0.36)		–/3.55	2.63	[32]
Zn-3p	286, 344	420 (0.81)		–/3.56	2.94	[32]
Zn-3q	279, 430	492, 544[e] (0.50)		–/3.49	2.50	[32]
Zn-3r	286, 326, 429	488, 513[e] (0.27)		–/3.49	2.55	[32]
Zn-3s	287, 330, 421	482, 512[e] (0.12)		–/3.38	2.57	[32]
Zn-4a	284, 321, 359, 415 (0.99)	513 (0.66)		5.75/3.16	2.59	[39]
Zn-4b	279, 325, 362 (2.74)	424 (0.43)		6.21/3.36	2.85	[39]
Zn-4c	288, 322, 392 (1.75)	443 (0.53)		6.14/3.36	2.78	[39]
Zn-4d	284, 331, 362, 397 (2.35)	446 (0.26)		5.90/3.17	2.73	[39]
Zn-4e	288, 324, 400, 485 (0.33)	586 (0.42)		5.30/3.22	2.08	[39]
Zn-4f	284, 317, 405 (2.69)	511 (0.31)		5.56/3.23	2.33	[39]
Zn-4g	284, 326, 411 (2.24)	518 (0.18)		5.91/3.40	2.51	[39]
Zn-4h	284, 337, 404 (9.07)	453, 470[e] (0.90)		5.88/3.12	2.76	[39]
Zn-4i	281, 320, 369 (11.25)	409[e], 432 (0.81)		6.22/3.31	2.91	[39]
Zn-5a	283, 316, 362	435 (0.38)	545 (0.35)	–/3.32	3.00	[43]
Zn-5b	283, 321, 371	421, 438[e] (0.31)	559 (0.26)	–/3.35	2.88	[43]
Zn-5c	284, 340, 397	440, 461[e] (0.41)	570 (0.37)	–/3.41	2.78	[43]
Zn-5d	283, 320, 370	449 (0.33)	528 (0.32)	–/3.31	2.95	[43]
Zn-6a	379	542 (1.3)	542			[44]
Zn-6b	381	503 (2.2)	487			[44]
Zn-6c	325	427 (0.37)	445			[44]
Zn-6d	379	510 (0.44)	467			[44]
Zn-6e	373	565 (0.33)	545			[44]

[a] Extinction coefficients ($\times 10^4$ g^{-1} dm^3 cm^{-1}) are shown in parentheses.
[b] Solution PL quantum yields are shown in parentheses.
[c] Film PL quantum yields are shown in parentheses.
[d] Minus sign is omitted for clarity.
[e] Shoulder peaks.

peak luminance of 2460 cd m^{-2} at 15 V.

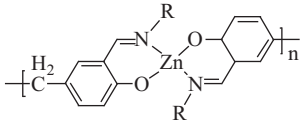

Zn-1

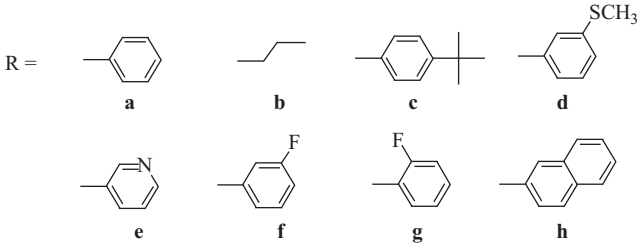

Apart from varying the attached groups on the nitrogen atom of the Schiff base unit, Cao and co-workers also reported the structure–property relationships of the polymers with different bridging spacer (Ar) in **Zn-2** [35]. By replacing the CH_2 unit in **Zn-1** with a conjugated aromatic ring in **Zn-2**, different absorption maxima were observed. The absorption maxima of **Zn-2a**, **Zn-2b** and **Zn-2c** were found at 358, 379 and 372 nm, respectively. Moreover, they emitted much stronger green fluorescence when excited by UV light. From **Zn-2a** to **Zn-2c**, the PL maximum is gradually red-shifted, which is consistent with an increasing effective π-conjugation length of the polymers using fluorene, carbazole and phenyl bridging unit (λ_{em} = 531, 540 and 546 nm, respectively). The Φ_{PL} of the neat polymer films are about 51, 46 and 42%, respectively, for **Zn-2a**, **Zn-2b** and **Zn-2c**. The PL efficiencies of these polymers are high and comparable to polyfluorene (~55%), and appear much higher than those polymers of **Zn-1**. The decrease of PL efficiencies from **Zn-2a** to **Zn-2c** follows the order of their PL properties

from fluorene to carbazole and benzene groups. PLEDs based on these polymers were fabricated and all the EL spectra matched the respective PL spectra with strong green emission maxima at 534, 541 and 548 nm, respectively, for **Zn-2a**, **Zn-2b** and **Zn-2c**. It should be noted that the EL efficiencies follow the same trend as PL efficiencies from **Zn-2a** to **Zn-2c**. Thus, an appropriate choice of the bridging ligands is a key criterion for obtaining highly efficient PLED materials. Therefore, zinc Schiff-base polymers provide a new entry to the development of polymeric materials for PLEDs.

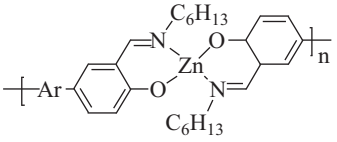

Zn-2

Ar =

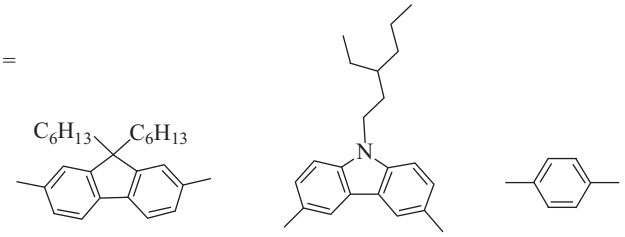

a **b** **c**

3.2. Zinc(II) terpyridine based polymers

In 1995, Constable et al. proposed that coordination polymers can be obtained by addition of metal ions to 2,2′:6′,2″-terpyridine (terpy) functionalized monomers [36]. Terpy-based coordination polymers containing Zn(II) template ions with perylene bisimide dyes were first synthesized by Würthner in 2002 [37]. The electronic communication between the transition metal-complexed moieties of π-conjugated bis- and tris(terpyridine)s points out their potential to be used as new functional optoelectronic materials. The terpy derivatives as chelating ligands form stable coordination compounds with Zn(II) ions via $d\pi \rightarrow p\pi^*$ bonding. This class of polymers exhibits charge-transporting properties with high thermal stability and flexibility in structural design and modification, rendering them important for uses in optoelectronic devices. In 2003, a detailed study of the structure–property relationships using this template was first carried out by the group of Che (**Zn-3a** to **Zn-3i**) [38]. A series of zinc(II) terpy-based polymers was synthesized by the reaction of rigid linear π-conjugated bis(terpyridine)s with zinc(II) acetate at a ratio of 1:1. Because of the filled *d*-electron shell, Zn(II) is not involved in any UV–vis transitions in such systems, therefore, only LC π–π^* or n–π^* transitions is observed between the Zn-terpy moieties and the chromophores. Therefore, electro-optical properties of the metallopolymers can be easily tuned with designed chromophores or π-conjugated spacer units. The absorption spectra of this type of polymers are similar to each other with the absorption maxima at 286–290 nm due to LC π–π^* transition of the aromatic moiety together with shoulders at 320–346 nm. The spacer between the terpy units mainly affects the λ_{em} and Φ_{PL} of the polymers. Taking the examples of **Zn-3a**, **Zn-3f**, **Zn-3g**, **Zn-3h** and **Zn-3i**, the film emission colors are blue, green, green, green and yellow, with λ_{em} (with the Φ_{PL} shown in bracket) = 450 (0.55), 546 (0.20), 530 (0.50), 535 (0.20) and 567 (0.55) nm, respectively. The polymers exhibit higher Φ_{PL} than their monomer counterparts. Detailed investigations were carried out by Schubert et al. a few years later by incorporating other aromatic donor as the bridge into the same system and by using these polymers in the fabrication of PLEDs (for **Zn-3j** to **Zn-3s**) [32]. They found that upon metallopolymerization, there is a shift of absorption wavelength because of the inductive effects caused by the metal ions, and a general decrease of the extinction coefficients caused by the hypochromic effect.

With different conjugated systems in terpy, a broad range of absorption and emission wavelengths are covered in **Zn-3j** to **Zn-3s**. The fluorene derivative (**Zn-3p**) is situated at the shortest-wavelength end of the absorption range (λ_{max} = 344 nm) followed by **Zn-3l** (λ_{max} = 373 nm). With an increase of effective π-conjugation length, the maximum wavelength of the absorption band becomes more red-shifted. Therefore, the metallopolymers with extended π-conjugated systems (i.e. **Zn-3n** and **Zn-3q** to **Zn-3s**) have their absorption maxima in the range of 420–450 nm. As a result, the shift of the absorption bands of the metallopolymers can be predicted by changing the type and extent of the π-conjugated system of the bis(terpyridine) subunits. Intense intraligand (IL) π–π^* or n–π^* blue to green emission bands (λ_{em} = 420–513 nm) have been observed for **Zn-3j** to **Zn-3s**. Metallopolymerization causes only marginal differences between the PL maxima of bis(terpyridine) ligand and the corresponding polymer. But, a decrease of Φ_{PL} accompanied by a significant broadening of the emission bands caused by aggregation or excimer formation was observed. There is a less pronounced aggregation of the PL spectrum if steric hindrance of the substituents was found on the bis(terpyridine) ligands as observed in **Zn-3m**, **Zn-3n**, **Zn-3p** and **Zn-3q**. The PL energy depends strongly on the size of the respective conjugated system. A significantly red-shifted emission toward the green (λ_{em} = 501 nm) has been observed in **Zn-3k** with increasing the effective π-conjugation length. The metallopolymer **Zn-3m** containing the unsymmetrical ligand displays an exceptional behavior showing its PL maximum at 468 nm.

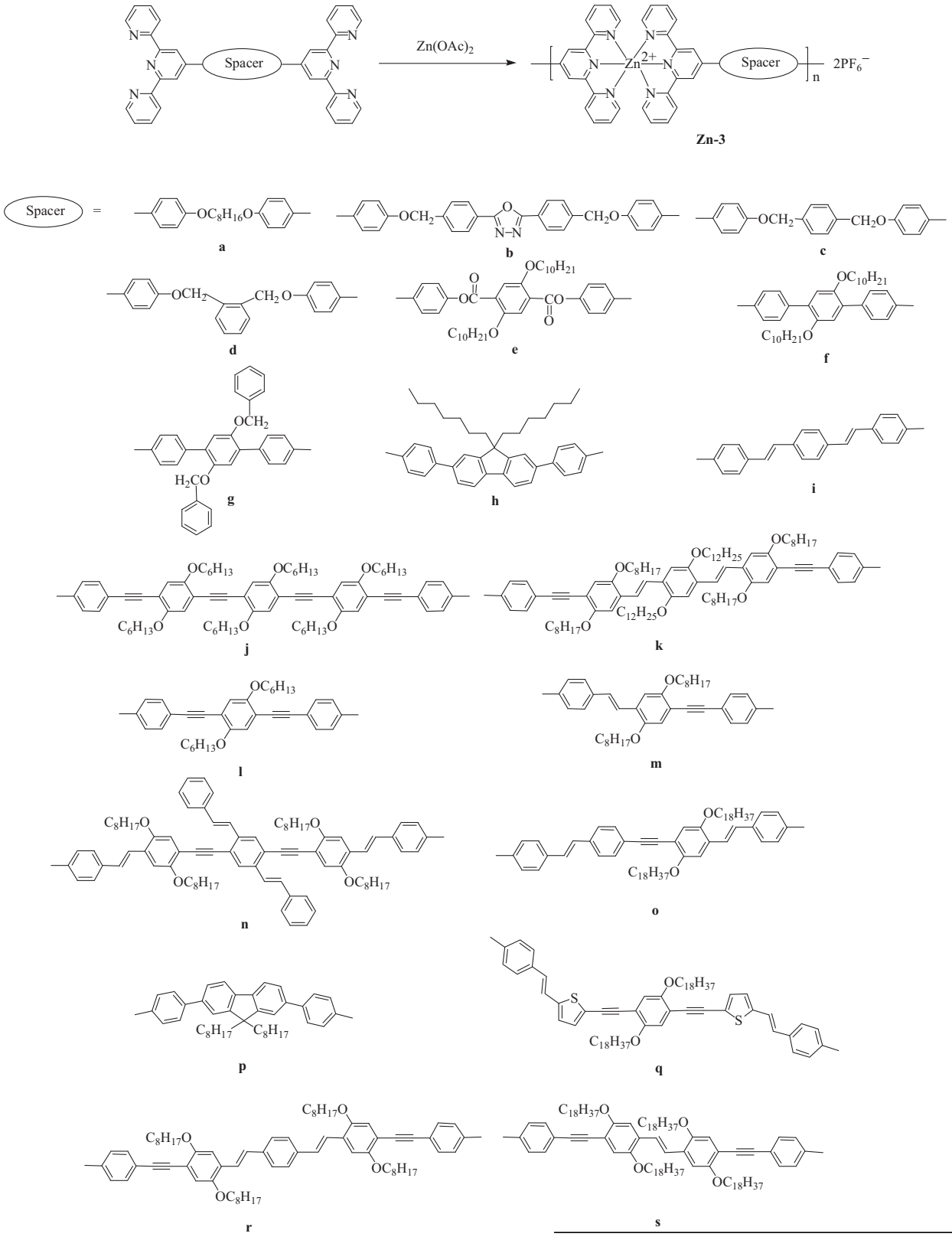

In continuation of this work, Schubert's group also reported a series of bis(terpyridine) derivatives bearing electron-accepting π-conjugated spacer units as the building blocks for the construction of Zn(II)-containing metallopolymers **Zn-4** [39]. This significantly influences the optical properties which can be tailored toward supramolecular low E_g materials, potentially good for photovoltaic applications [40]. Fig. 2 displays the influence of bandgaps on Zn terpy-based polymers by different spacer groups. For Zn-based metallopolymers with electron-donating spacer units, a charge-transfer (CT) between electron-rich central unit and the metal-coordinated electron-deficient terpy unit causes a red-shift in the absorption features. In the acceptor

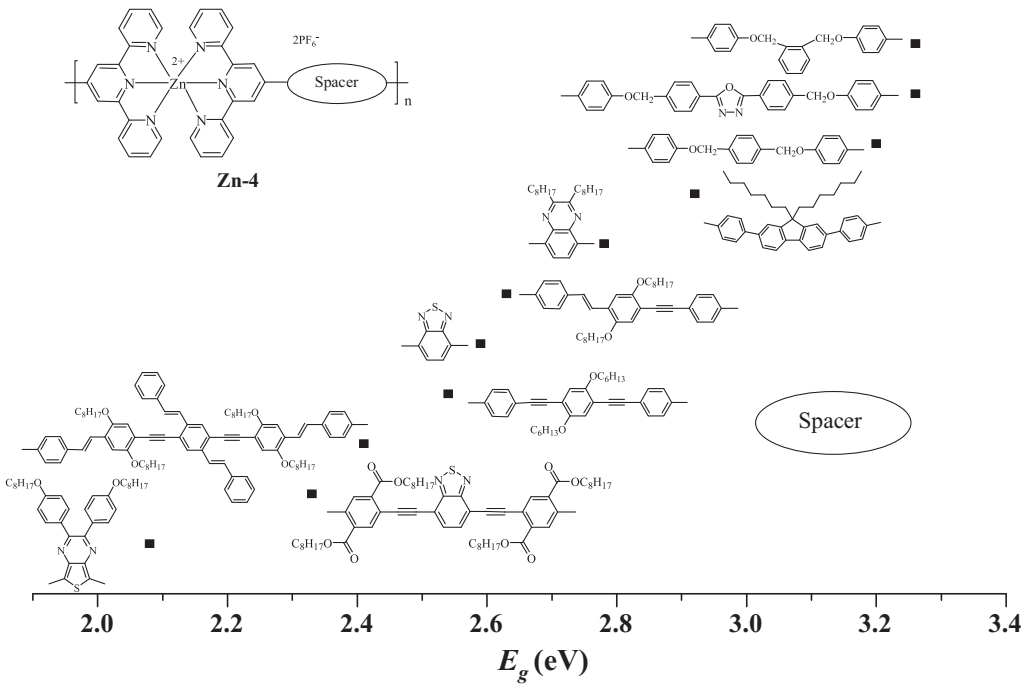

Fig. 2. Optical bandgaps for zinc(II) terpyridine based polymers with different spacer groups (see Ref. [32,38,39]).

cases, the central chromophores consist of electron-withdrawing groups which are not able to undergo such CT processes with the terpy units. Inductive effects, which are caused by the complexed metal ion, do not compensate for the missing CT band, thus leading to a small blue-shift of the absorption bands. Additionally, the UV–vis absorption data of the metallopolymers revealed a considerable decrease of the extinction coefficients values, which may be attributed to a parallel arrangement of the dipole moments of the bis(terpyridine) units within the polymer backbone. Polymer **Zn-4e** bearing strongly electron-withdrawing thieno[3,4-*b*]pyrazine exhibits the longest absorption wavelength (λ_{max} = 485 nm) and, therefore, the smallest gap between the HOMO and LUMO energy levels (E_g = 2.08 eV). On the other hand, **Zn-4b** with 2,5-dimethylterephthalic acid dioctyl ester possesses the lowest absorption wavelength (λ_{max} = 362 nm), corresponding to the largest HOMO–LUMO energy gap (E_g = 2.85 eV). Depending on the effective π-conjugation length and push–pull effects of the ligands, a wide range of PL emission wavelengths are available. These metallopolymers exhibit higher absolute Φ_{PL} than the conventional π-conjugated organic polymers bearing similar backbone units reported in the literature. For instance, there is a 3-fold increase in Φ_{PL} for **Zn-4e** ($\Phi_{PL} \sim 0.42$) relative to the organic polymers with thieno[3,4-*b*]pyrazine unit ($\Phi_{PL} \sim 0.15$ in solution) [41]. Compared to the Φ_{PL} values of [2,1,3]benzothiadiazole and quinoxaline-bearing π-conjugated organic polymers of about 0.19 and 0.22, respectively [42], metallopolymers **Zn-4a** and **Zn-4c** (Φ_{PL} = 0.66 and 0.53) emit light much more efficiently.

Polymers with a combination of electron acceptors and electron donors **Zn-4** were also synthesized in which relaxation of the excited state by emission occurs via a transfer of energy from the excited donor part to the acceptor moiety. The absorption spectrum of **Zn-4h** shows a good conformity with individual spectra of the homopolymers but this is not the case for the extinction coefficients. The photophysical properties of selected homopolymers are displayed in Fig. 3.

Zn(II)-terpy polymers **Zn-5** were proposed by Lin and coworkers [43]. Comparing **Zn-3h** and **Zn-5a**, adding triple bonds throughout the polymer chains did not exert any influence on the optical effect and their photophysical properties are similar. The substituents on the phenylene cores lead to a shift in the absorption and emission maxima. For the longest-wavelength absorption peaks, the λ_{max} values follow the order of **Zn-5c** (OMe) > **Zn-5b** (Me) > **Zn-5a** (H). When a strong electron-donating OMe group is laterally attached to the conjugated core, the CT transition state is progressively shifted toward the lower energy. Good external quantum yields (EQEs) between 0.36 and 1.02% and the maximum brightness between 323 and 931 cd m^{-2} at 14 V were recorded when polymers **Zn-5b** to **Zn-5d** were used in PLED fabrication.

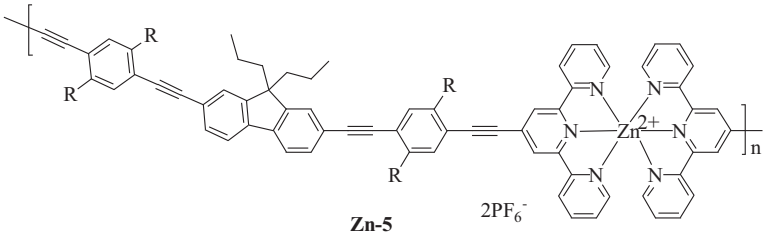

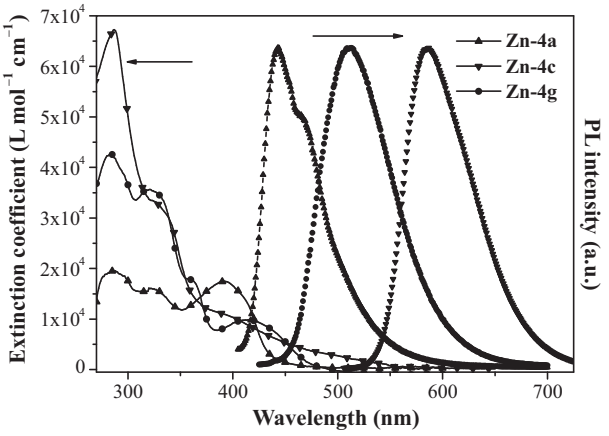

Fig. 3. Absorption (solid line) and normalized PL spectra (dashed line) of selected Zn homopolymers in 10^{-6} M DMF at room temperature (see Ref. [39]).

3.3. Zn(II)-containing side chain polymers

A family of Zn-containing side chain polymers was also reported [44]. The polymers retain full solution processability but better injection efficiency, lower operating voltage and higher quantum yield than the widely used tris(8-hydroxyquinolinato)aluminum (Alq_3). This type of polymer was synthesized by ring opening metathesis polymerization with different functionalization of the monomers. The solution emission of polymers can be tuned from blue (427 nm) to yellow (565 nm) through simple variation of the second functionalized quinoline unit. These results clearly demonstrate that the fluorescence properties of the material can be modulated with ease in solution and the polymer backbone does not interfere with the optical properties of the zinc luminophore. The monomer ratios in copolymers also affect the emission wavelength. The 1:1 copolymer emission is red-shifted in comparison to the emission of the 1:20 copolymer. The emission wavelength is also dependent on the packing of the quinolate ligand. The shorter the interligand contacts, the more red-shifted the emission is. Regardless of the luminophore concentration and the quinoline ligand used, the emission data of the thin films again indicate that the polymer backbone does not inhibit fluorescence, even in the solid state.

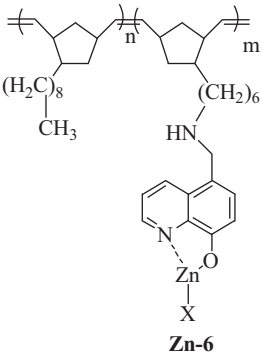

Zn-6

X =

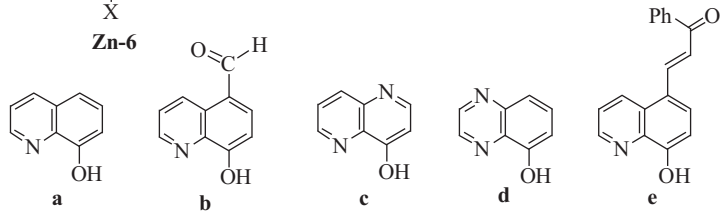

a **b** **c** **d** **e**

4. Ruthenium-containing polymers

Ruthenium(II) complexes are among the most studied molecules due to their rich and well characterized photophysics and redox chemistry (Table 2) [19,45,46]. The polymers derived from these complexes have potential to excel for applications in sensor, polymer supported electrode, nonlinear optics, photo-refraction and EL devices [10–13,46]. Among these, they are effective in the conversion of solar radiation into chemical energy, hence providing clean and renewable energy sources.

4.1. Conjugated polymers with $Ru(bpy)_2$ moieties on the main chain

Since its discovery at the end of the 19th century, 2,2′-bipyridine (bpy) and its derivatives have been widely used in the complexation of metal ions due to the robust redox stability and ease of functionality of bpy. Before a Ru(II) ion coordinates to the bpy-based polymer, the unmetalated polymer conjugation is disrupted by the inter-ring twisting at the bpy moiety. However, upon Ru coordination to the bpy unit, the non-planar bpy units are forced into a syn-planar conformation that effectively increases the effective conjugation length. The increased conjugation length changes the photophysical properties (e.g. red-shifted absorption with higher intensity of the low-energy bands, red-shifted emission bands and lower E_g) and signals the presence of the coordinated metal ion. There are two types of coordination of Ru complexes to the polymer chain. Bpy ligands are either directly embedded into π-conjugated polymer backbone or tethered with the polymer backbone as a pendant group via conjugated or non-conjugated linker.

Yamamoto and co-workers have synthesized the first fully conjugated polymers **Ru-1** that contain ruthenium chromophores which are incorporated into the polymer backbone via the bpy coordinating unit. In this work, bpy and 5,5′-bipyrimidine (bpym) units were utilized as the post-polymerization metal coordination sites [47]. Controlled polymerization (chain length ~ 10 repeating units) is needed in order to preserve a good solubility of the polymers. **Ru-1a** exhibits a metal-to-ligand charge transfer (MLCT) absorption band at 450 nm, a $\pi-\pi^*$ transition band due to the bpy polymeric backbone at 360 nm and a $\pi-\pi^*$ absorption due to the ancillary bpy ligands at 290 nm. The PL of **Ru-1a** has λ_{max} = 694 nm, which is red-shifted compared to that of the parent complex, $[Ru(bpy)_3]^{2+}$ (λ_{max} = 612 nm). Clearly, there is energy transfer between the bpy backbone and the Ru chromophore. The absorption spectrum of bipyrimidine-based polymer **Ru-1b**

Table 2
Photophysical properties of Ru(II)-containing polymers.

Polymer	Feed ratio [mol.%]	$\lambda_{max,abs}$ [nm]	$\lambda_{em,PL(sol)}$ [nm]	$\lambda_{em,PL(film)}$ [nm]	HOMO/LUMO[a] [eV]	Ref.
Ru-1a		290, 360, 450	694			[47]
Ru-1b		285, 435				[47]
Ru-2		500–520				[48]
Ru-3a		450, 550				[49]
Ru-3b		550				[49]
Ru-4		550–700				[50]
Ru-5		390, 460, 600[b]				[51]
Ru-6		410–450, 500				[52]
Ru-7						[52]
Ru-8a		290, 476	629			[53]
Ru-8b		287, 464	770			[53]
Ru-9a		335, 365, 565			6.3/3.3	[54]
Ru-9b		310, 356, 372, 492			6.3/3.3	[54]
Ru-10		507			6.4/4.0	[55]
Ru-11a		286, 312, 496		652, 766, 810		[56]
Ru-11b		286, 310, 494		660, 765		[56]
Ru-11c		286, 310, 492		666, 760, 785		[56]
Ru-11d		286, 312, 494		668, 750		[56]
Ru-11e		288, 312, 492		675, 752		[56]
Ru-11f		286, 310, 494		652, 752, 800		[56]
Ru-12				680–700		[11]
Ru-13a	$x = 0.1$; $y = 0.9$	290, 315, 452, 498	575, 610, 625			[57]
	$x = 0.2$; $y = 0.8$	288, 315, 444, 500	550, 578, 606, 630			
Ru-13b	$x = 0.1$; $y = 0.9$	288, 450, 496	575, 620			[57]
	$x = 0.2$; $y = 0.8$	288, 452, 500	575, 620, 640			
Ru-14		425, 480	642			[58]
Ru-15a		346, 412, 590, 700[b]			4.9/2.8	[59]
Ru-15b		346, 412, 590, 700[b]			4.9/2.8	[59]
Ru-16		300, 456				[60]
Ru-17a						[62]
Ru-17b		454		605		[63]
Ru-18		280–340, 509	350, 370, 466			[61]

[a] Negative sign is omitted for clarity.
[b] Absorption tail.

features an MLCT band at 435 nm and a π–π^* transition band due to the ancillary bpy at 285 nm. A long tailing absorption on the red side of the MLCT band suggests the existence of 1:2 complexes where two metal units are coordinated to a single bpym unit (i.e. $[(bpy)_2Ru(\mu\text{-bpym})Ru(bpy)_2]^{4+}$). This polymer is, however, non-photoluminescent.

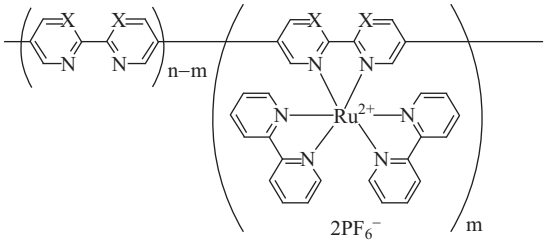

Ru-1 X = C **a**
X = N **b**

Chan and co-workers reported poly(benzobisoxazole)s (**Ru-2a** and **Ru-2b**) and poly(benzobisthiazole)s (**Ru-2c** and **Ru-2d**) that contain $[Ru(bpy)_3]^{2+}$ units [48]. Spectroscopy studies show that when 2,2-bipyridine-5,5-diyl group is incorporated in the polymer backbone, the electronic delocalization is more extended than that when the 2,2-bipyridine-4,4-diyl unit is used. The absorption bands centered at 500–520 nm in the spectra of the polymer–metal complex hybrids are assigned to the MLCT transitions. Coordination of Ru to these polymers does not change the position of the π–π^* transitions of the conjugated backbone. An emission band at 530 nm and a shoulder at 580 nm are attributed to the conjugated π–π^* and MLCT states, respectively. Incorporation of the Ru ion into these polymers dramatically increases the charge carrier mobility showing that the Ru complexes can improve the charge transport through the polymeric material.

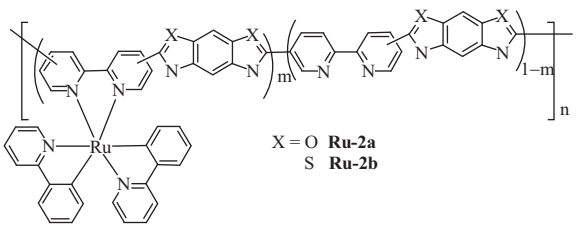

X = O **Ru-2a**
S **Ru-2b**

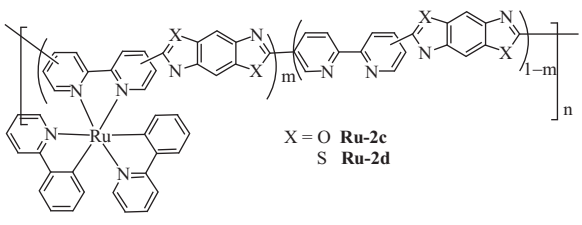

X = O **Ru-2c**
S **Ru-2d**

Yu and co-workers have synthesized the first poly(*p*-phenylene vinylene)s (PPV) containing Ru(II) chromophores which are incorporated into the polymer backbone via the bpy coordination unit [49]. The absorption spectrum of **Ru-3a** exhibits a composite of the properties of the metalated and unmetalated polymers with λ_{max} = 450 nm. The all-Ru polymer **Ru-3b** shows an intense π–π^* absorption at 550 nm, which is significantly red-shifted from **Ru-3a** and the parent $[Ru(bpy)_3]^{2+}$ complex. The absorption strength of the polymers at the longer wavelength can be adjusted simply by controlling the ratio of the monomers. This is a useful feature for controlling the optical properties of polymers. However, unlike the Ru-monomer and organic-based polymers, these types of Ru polymer are non-emissive in nature. To further tune the optical and electronic properties of these metal–organic PPV materials, structurally similar PPV polymers that incorporate Ru complexes with different diketonate and hydroxyquinoline ligands (**Ru-4**) were also synthesized by the same group [50]. The replacement of diketonate and hydroxyquinoline groups in the ancillary ligands on Ru substantially lowers the Ru(II/III) redox potential relative to the analogous polypyridyl complexes. This lowering of the Ru(II/III) potential induces a significant red-shift in the Ru → bpy-PPV MLCT transition. Consequently, in polymers **Ru-4**, the MLCT transition is clearly located as a weak band in the 550–700 nm region. Side chain attachment of a donor–acceptor (D–A) type stilbene derivative which acts as the nonlinear optical chromophore did not cause much inferior effect on the optical properties in **Ru-5** [51].

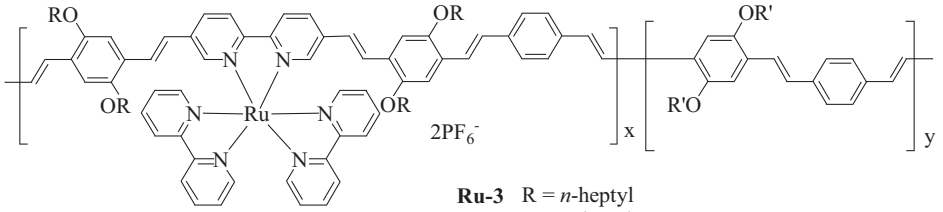

Ru-3 R = *n*-heptyl
R' = *n*-hexyl
x = 0.1, y = 0.9 **a**
x = 1, y = 0 **b**

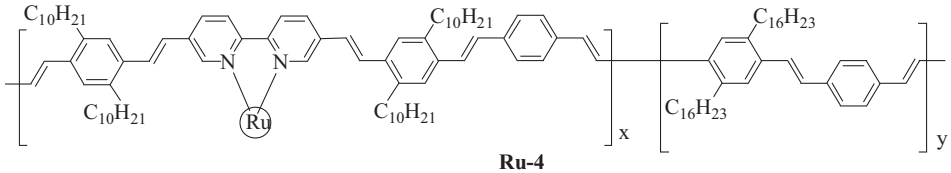

Ru-4

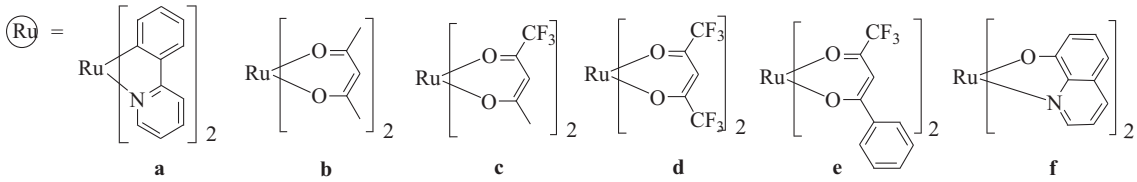

a **b** **c** **d** **e** **f**

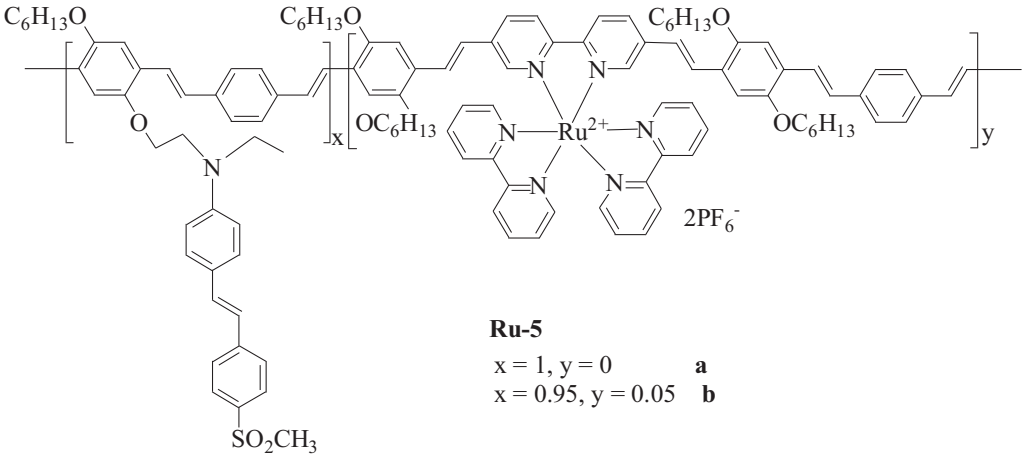

Ru-5
x = 1, y = 0 **a**
x = 0.95, y = 0.05 **b**

The use of Ru-containing polymers as light emitter was reported by Chan et al., in which electron-transporting and hole-blocking aromatic oxadiazoles were introduced into the PPV system (**Ru-6**) [52]. The oxadiazole units can be introduced either at 5,5′- or 4,4′-position. Similar to the polymers aforementioned, all these polymers exhibit three absorption bands due to the π–π* IL absorption band at 290 nm of the bpy ligands, π–π* transition of the conjugated main chain (410–450 nm) and MLCT transition of the Ru complex at approximately 500 nm. The absorption maxima of the latter two bands are shifted to the shorter wavelengths but with higher intensity when the metal content is increased. Therefore, it is feasible to tune the optical properties and charge carrier mobilities of the polymers by changing the metal content in order to meet the target optoelectronic applications. Conjugated polymers with oxadiazole moieties exhibit improved light-emitting device performance because of the balanced charge injection from both electrodes. Polymer **Ru-7** with 1,10-phenanthroline ligand displays similar optical properties as **Ru-3**.

Guillerez et al. conducted a detailed photophysical investigation of polythiophene-based Ru conjugated polymers. Polymers **Ru-8** that contain regioregular 3-(octylthiophene) tetramers or hexamers alternating with $[Ru(bpy)_3]^{2+}$ have been reported [53]. The absorption spectrum of **Ru-8b** exhibits many similar features as that of **Ru-8a**; however, the dominant low-energy band of **Ru-8b** displays an enhanced molar absorptivity per repeat unit and an increased absorption bandwidth. The increase in absorptivity is caused by the increase in the number of thiophene rings in the repeat unit. The increased bandwidth may be due to the longer thiophene segment length, which allows for a greater number of conformations, leading to an increased distribution of π–π* transition energies. These two polymers are weakly emissive only, and **Ru-8a** has a similar energy and band shape relative to that for $[Ru(bpy)_3]^{2+}$. **Ru-8b** features an exceedingly weak emission at λ_{max} = 770 nm. This emission is red-shifted and considerably weaker (by ca. 20-fold) compared to the emission of **Ru-8a**.

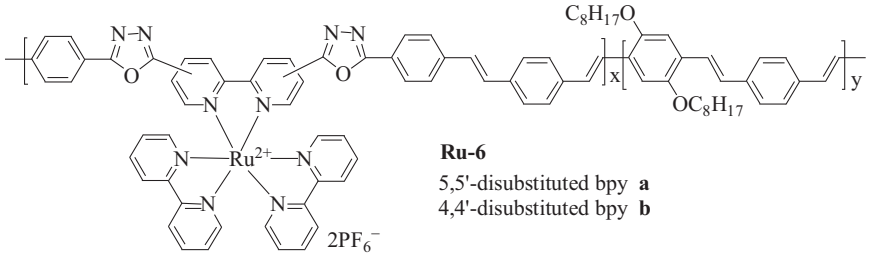

Ru-6
5,5'-disubstituted bpy **a**
4,4'-disubstituted bpy **b**

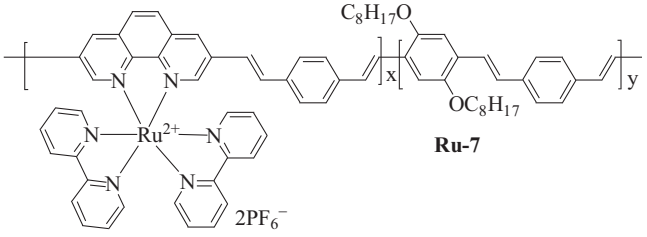

Ru-7

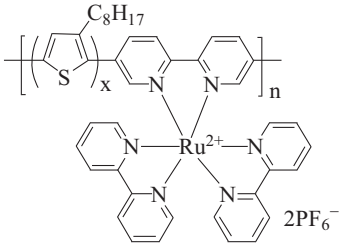

Ru-8
x = 4 **a**
x = 6 **b**

Another example of main-chain Ru-containing polymer goes to **Ru-9** with tridentate 2,6-bis(benzimidazol-2-yl)pyridine ligand [54]. After the formation of the polymer–metal complexes, an extra absorption peak was observed beyond 490 nm, but the transition energy is higher than that in the case of bpy because of the less extended conjugation in the polymer main chain. The absorption of benzimidazolyl analogue **Ru-9a** (λ_{max} = 335, 365, 565 nm) is more red-shifted than that of benzothiazolyl species **Ru-9b** (λ_{max} = 310, 356, 372, 492 nm). The main chain transitions at ca. 360 nm are preserved but the vibronic structures can be resolved in **Ru-9b**.

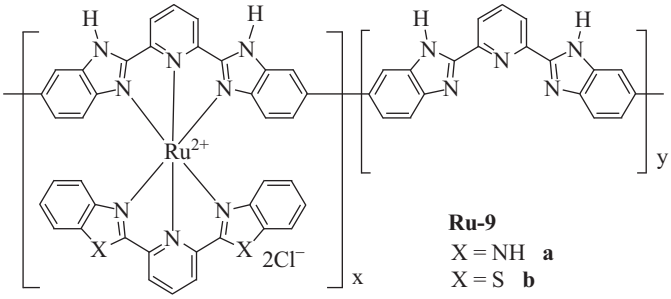

Ru-9

4.2. Non-conjugated Ru-containing polymers with rigid main chain

Here, conjugation is disrupted by metal complexes (e.g. Ru-terpyridines), amides or imides. Therefore, the absorption and emission features appear as those from individual fragments of the polymer chain. **Ru-10** displays similar absorption pattern to the monomer (MLCT transition at λ_{em} = 507 nm) [55]. Unlike the polymers of **Ru-3** which exhibit main-chain π–π* absorption bands at ~450 nm, such absorption was not observed in **Ru-10** because the orthogonal geometry between the two terpy ligands and the π-conjugated system on the polymer main chain is disrupted. The photovoltaic properties of the devices based on this polymer were studied, resulting in the power conversion efficiency (PCE) of the order of 10^{-3}% and the incident photon-to-electron conversion efficiency (IPCE) was 2% at 510 nm.

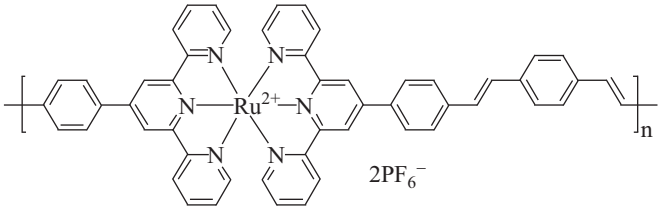

Ru-10

Chan's team also prepared a family of polyimides based on Ru(II)-terpy complex (**Ru-11**) [56]. All polyimides show very similar absorption features as dominated by the electronic transitions due to the Ru-terpy complexes and analogues to **Ru-10**. The bands centered at ca. 286 and 310 nm correspond to the LC transitions of the terpy moieties. Another absorption at approximately 500 nm is ascribed to the MLCT ($Ru^{2+} \rightarrow$ terpy) transitions. They all exhibit two major film emission bands in the vicinities of 650 and 750–800 nm. Unlike other Ru-polymers, which are non-luminescent in solution state or have very short lifetimes at room temperature, solution PL spectra of **Ru-11** give rise to one emission band at ca. 600–650 nm originating from the emission of the MLCT states. The shape and intensity of the MLCT emission bands vary with different polymers, probably due to the structural differences in the diimide unit.

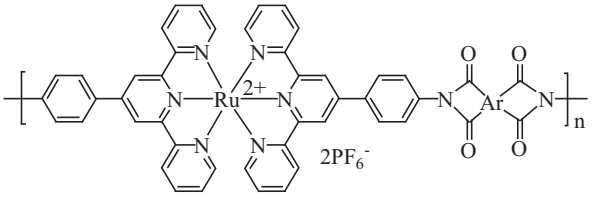

Ru-11

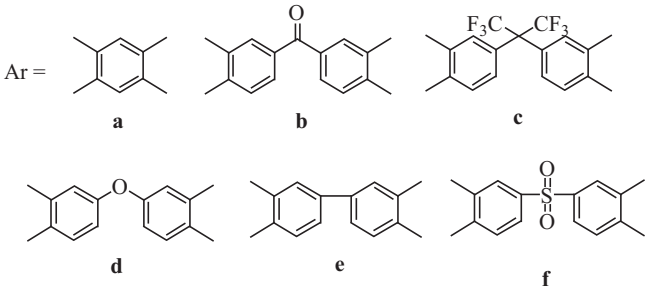

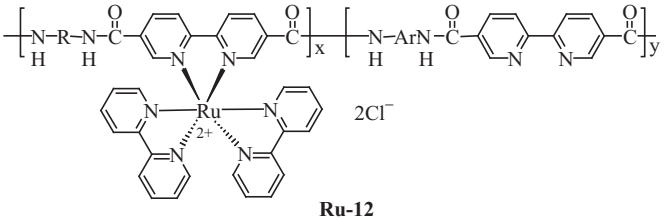

Ru-12

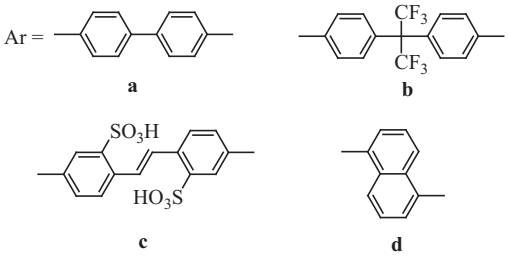

The synthesis of different aromatic polyamide with 2,2′-bipyridyl moieties (**Ru-12**) was also reported [11]. In this case, the emission of the polymers is dominated by the emission from $[Ru(bpy)_3]^{2+}$ MLCT excited state and they all showed an emission band centered at ca. 680–700 nm. These observations indicate that the emissions from the MLCT states are not affected by changing the diamine monomers or by the ratio of the monomers. This may be due to the non-conjugated feature throughout the polymer chain. However, the thermotropic and lyotropic properties of the polymer are affected by the choice of monomers.

4.3. Conjugated polymers with Ru moieties on the side chain

In this section, the Ru(II) complexes are attached as side chain chromophores which are non-conjugated to the main chain polymers. If the main chain is a luminescent conjugated polymer, both the metal complex and polymer may function as the light emitter and they do not influence each other in most cases. The absorption spectra show the bands due to the π–π* transition of bpy or terpy, followed by conjugated main chain absorption bands and the MLCT transition of Ru complexes. **Ru-13** belongs to a series of PPV polymers with pendant $[Ru(bpy)_3]^{2+}$ or $[Ru(terpy)_2]^{2+}$ [57]. The UV–vis absorption spectra of the polymers show intense absorption bands due to both the conjugated main chain and the Ru moieties. Their PL spectra are dependent on the metal complex

content. When the polymer contains 10% $[Ru(bpy)_3]^{2+}$ per repeating unit, emissions from both main chain and metal complex can be observed. However, when the Ru core content is increased to 20%, the emission from the main chain is partially quenched by the Ru complex, which has lower-lying $d\pi^*$ MLCT excited states rather than the π–π^* excited state of the main chain. The Ru content in the polymers also affects the shape of the EL spectra. Two emission bands at 560 and 650 nm were observed in **Ru-13a** and their relative intensities would change as the Ru content is increased to 20% at which the peak at 650 nm becomes dominant. Similar emission properties were also observed in **Ru-13b** except that the peak of the MLCT emission is shifted to 680 nm with 10% Ru content. However, when the Ru content in **Ru-13b** is increased to 20%, only a single peak was detected at 690 nm. The difference in **Ru-13a** and **Ru-13b** at high Ru content is believed to be due to the notion that Ru(tpy) complex is not an efficient quencher compared to the bipyridyl analogue.

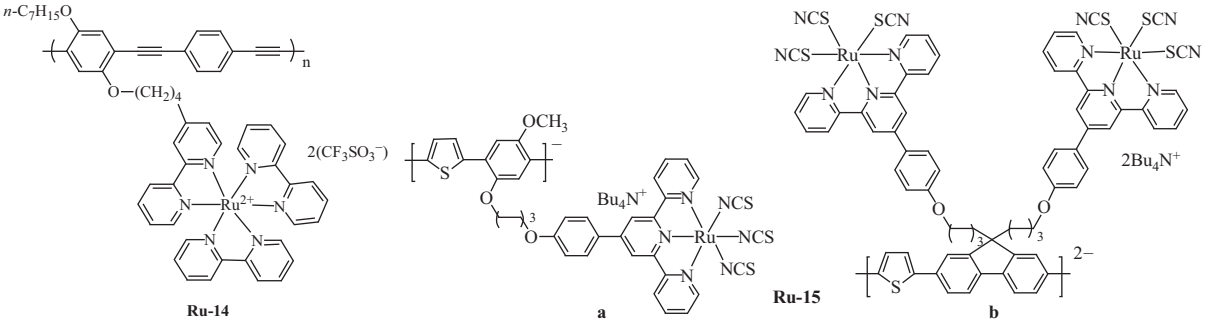

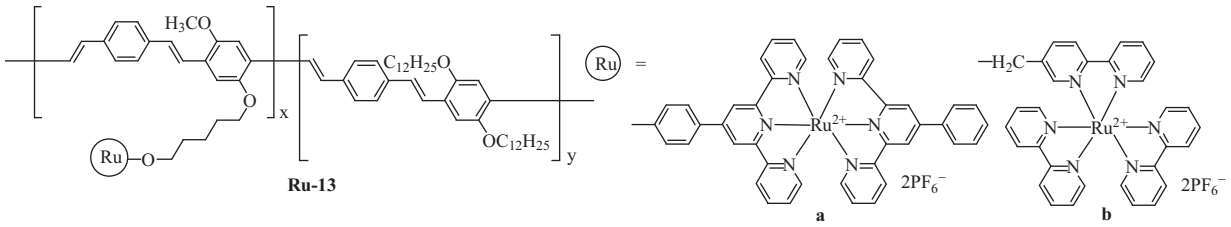

Conjugated polyyne **Ru-14** displays an intense absorption band at 425 nm due to the long-axis polarized π–π^* transition of the acetylide fragment [58]. Weaker absorptions in the 450–500 nm region arise from metal to bpy MLCT transition. The polymer features a broad luminescence with λ_{em} = 642 nm due to the Ru → bpy MLCT excited state. Similar observation was found in **Ru-15** [59], in which π–π^* absorption bands due to the IL and conjugated main chain transitions are all consistent with the results. However, by replacing one of the terpy ligands with trithiocyanate system, the MLCT bands show dominant bathochromic shift and are centered at 590 nm which extend beyond 700 nm. It is believed that the presence of the three thiocyanate ligands would stabilize the excited state by electron donation to the Ru center. Therefore, by simply changing the ancillary ligands on the Ru complex, the absorption in the near IR region was enhanced and photons with lower energy can be absorbed more efficiently. The identical optical properties between **Ru-15a** and **Ru-15b** provide good evidence that metal complexes and main chain polymer absorb and emit light separately. So, individual modification of the polymer main chain and Ru complex is critical in order to optimize the optical properties. A photovoltaic device fabricated from **Ru-15a** exhibits a higher short-circuit current J_{sc} (2.58 mA cm^{-2}) and the fill factor (FF) is 0.38, which is slightly higher than the devices fabricated from **Ru-15b** (J_{sc} = 1.60 mA cm^{-2}; FF = 0.29).

4.4. Non-conjugated polymers with Ru moieties on the side chain

The absorption and emission properties of Ru side-chain polymers with non-conjugated main chain (**Ru-16** to **Ru-18**) arise solely from the Ru complexes. All of these polymers exhibit absorption due to the MLCT transition of the Ru complexes. Being incorporated with charge transport units including triphenylamine and carbazole (**Ru-16** [60] and **Ru-18** [61]), poly(ethylene glycol) (**Ru-17a**) [62] or methyl methacrylate (**Ru-17b**) [63], the thermal, physical and charge transport properties of the polymers would vary but the optical properties remain relatively unchanged. Increasing the amount of metal complexes in **Ru-18** would result in an increase of the MLCT contribution in the absorption spectrum while the absorption intensity due to the carbazole unit remains essentially the same.

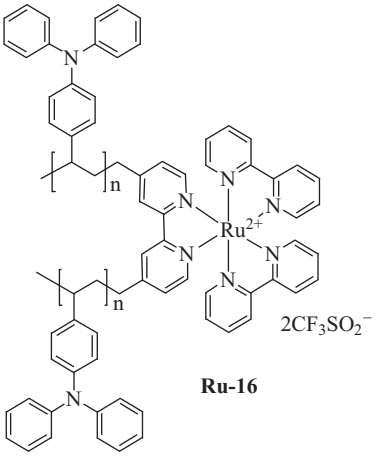

Ru-16

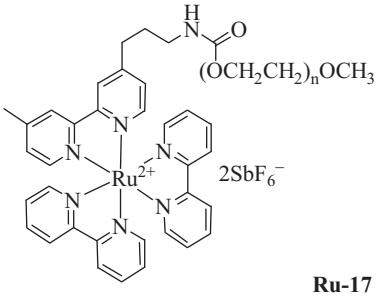

a

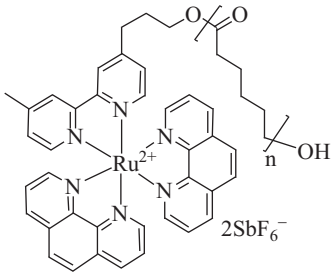

Ru-17

b

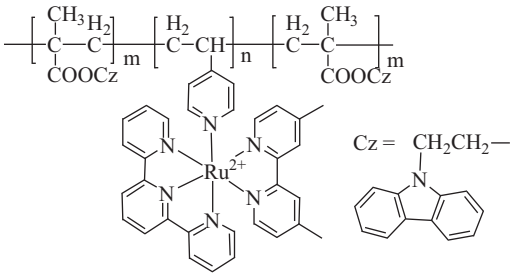

Ru-18

n = 0, 2, 4, 10, 14, 20
m = 20–22

5. Iridium(III)-containing polymers

As one of the most promising optoelectronic materials, polymers that contain phosphorescent Ir(III) complexes have attracted increasing attention in recent years. They represent a class of well known electroluminescent materials with excellent device performance. Phosphorescent PLEDs can be realized by doping phosphorescent dyes into a suitable polymeric host. Although the devices fabricated by this method have successfully exhibited outstanding performances, they typically suffer from phase separation, which leads to a fast reduction of efficiency with increasing current density. An efficient solution to this problem is to introduce Ir(III) complexes into the polymer side- and/or main-chain by means of a chemical bond in order to limit the interaction among guest chromophores and thereby reduce triplet–triplet annihilation upon device operation at high current density. So far, efficient green-, red- and white-emitting PLEDs based on polymers with main-chain Ir(III) complexes have been realized successfully.

Phosphorescent Ir(III) polymers are often composed of two components, namely the polymer host and the Ir(III) complex guest. Both functional units would affect the overall PL and EL of the resulting polymers. For the polymer host, it can be conjugated or non-conjugated in nature. The conjugated host polymer mostly contains highly fluorescent and charge transporting polyfluorene as the blue emitter and high triplet energy and excellent hole-transporting carbazole. For non-conjugated hosts, most of them are poly(*N*-vinylcarbazole) (PVK) and its derivatives and they have high-energy blue-emissive singlet excited state, favorable film-forming properties and durability at high temperature and excellent hole mobility. For the phosphorescent Ir(III) complex guest, optimizing the ligand structures and the relative amount of Ir content in the polymer would greatly affect the color and device performance of the resulting polymers. Table 3 collects the photophysical data for some Ir-containing polymers.

5.1. Conjugated polymers with Ir(III) complexes on the main chain

Conjugated polymers with Ir complexes in the main chain can be divided into three types, Ir complexes anchored with C^N, N^N or O^O ligands. The PL properties of these Ir polymers can be varied by different approaches.

5.1.1. Conjugated polymers with a C^N or N^N ligand of Ir complexes on the main chain

Under this category, the complexes are directly attached to the polymer backbones via ligands that are integral parts of the aromatic main chain. Full conjugation of the main chain was preserved if the C^N or N^N ligands are two-way attached by Suzuki coupling between dihalogenated Ir complexes and other aromatic monomers. Generally, the absorption bands of the metal units in copolymers are red-shifted, indicating that the complexes are conjugated with the polymer backbones. Langecker and Rehahn reported polyfluorene functionalized with some Ir green emitters (**Ir-1** and **Ir-2**) [64]. Similar optical behavior was found in both polymers. Their absorption spectra are dominated by the characteristic absorptions of the polyfluorene backbone at $\lambda_{max} \sim 230$ and 350 nm. Only a minor contribution of the Ir complexes was found in the λ_{max} range of about 300–430 nm. This contribution slightly increases with increasing the relative content of Ir complexes. Their film PL spectra show very minor emissions at around 420 and 450 nm, and are dominated by very strong phosphorescent signals of the Ir complexes ($x = 0.1$ at 600 and 630 nm), but the emission pattern appears in a reverse manner in their solution state. If the Ir content decreases from $x = 0.1$ to 0.02, incomplete energy transfer from the fluorene moieties to the Ir complexes would lead to higher emission intensity in the higher energy region, and the overall color of the polymer would be changed. A change of the color of the Ir polymer (red) from the Ir monomer (green) was attributed

Table 3
Photophysical properties of Ir(III)-containing polymers.

Polymer	Feed ratio [mol.%]	$\lambda_{max,abs}$ [nm]	$\lambda_{em,PL(sol)}$ [nm]	$\lambda_{em,PL(film)}$[a] [nm]	HOMO/LUMO[b] [eV]	E_g [eV]	Ref.
Ir-1	x = 0.02	230, 350;	400–500	420, 450[c]			[64]
	x = 0.05	300–430	600[c]	600, 630			
Ir-2	x = 0.02	230, 350;	400–500	420, 450[c]			[64]
	x = 0.05	300–430	600[c]	600, 630			
Ir-3	x = 0.1			600–610	4.50/3.20	2.2	[65]
Ir-4a	x = 1	350		410, 575 (0.25)			[66]
	x = 2	350		410, 575 (0.35)	5.56/2.50	3.06	
	x = 5	350		585 (0.34)	5.53/2.50	3.03	
	x = 10	350, 480		585 (0.12)	5.50/3.00	3.00	
Ir-4b	x = 1	350		410, 575 (0.31)	5.5/3.05	3.05	[66]
	x = 4	350		575 (0.21)	5.50/3.04	3.04	
	x = 10	350, 485		575 (0.17)	5.46/2.98	2.98	
	x = 20	350, 485		580 (0.06)	5.38/2.95	2.95	
Ir-5	x:y:z = 24:24:2	382	418	467 (0.013)	5.42/2.30	2.92	[67]
	x:y:z = 22.5:22.5:5	368	418	583 (0.006)	5.45/2.50	2.92	
	x:y:z = 20:20:10	372	418	577 (0.003)	5.43/2.51	2.92	
	x:y:z = 20:10:20	343	419	582 (0.005)	5.44/2.51	2.93	
	x:y:z = 48:0:2	344	409	414 (0.055)	5.41/2.31	3.10	
	x:y:z = 45:0:5	347	410	568 (0.02)	5.46/2.36	3.10	
	x:y:z = 40:0:10	345	410	568 (0.024)	5.43/2.33	3.10	
	x:y:z = 30:0:20	345	410	568 (0.021)	5.45/2.33	3.10	
Ir-6a	x = 1	260, 310		532, 574 (0.26)			[68]
	x = 3	270, 320, 420		532, 574 (0.20)			
	x = 5	270, 320, 420		532, 574 (0.25)			
Ir-6b	x = 3	260, 310, 430		531, 567 (0.34)			[68]
	x = 5	260, 310, 430		531, 568 (0.62)			
Ir-6c	x = 3	260, 330, 420		531, 569 (0.27)			[68]
Ir-7	x = 5	350, 450		560, 601 (0.09)			[68]
Ir-8				420, 520, 660, 720			[69]
Ir-9				420, 530, 625			[70]
Ir-10	q = 0.5			624 (0.061)	5.80/2.19	3.61	[71]
	q = 2			625 (0.05)	5.80/2.20	3.60	
	q = 4			628 (0.047)	5.78/2.22	3.56	
	q = 8			629 (0.035)	5.77/2.23	3.54	
	q = 16			631 (0.031)	5.76/2.25	3.51	
Ir-11	m = 50, n = 49.5, q = 0.5			617 (0.023)	5.18/2.39	2.79	[72]
	m = 50, n = 48, q = 2			619 (0.041)	5.19/2.40	2.79	
	m = 50, n = 46, q = 4			622 (0.054)	5.21/2.36	2.85	
	m = 50, n = 42, q = 8			618 (0.02)	5.18/2.28	2.90	
Ir-12	n = 0.1			632 (0.138)	5.36/1.78	3.58	[73]
	n = 0.2			632 (0.057)	5.35/1.77	3.58	
	n = 2			631 (0.047)	5.34/1.77	3.57	
	n = 4			635 (0.042)	5.34/1.78	3.56	
Ir-13	n = 2			638 (0.075)	5.13/1.52	3.61	[73]
Ir-	z = 0.5			620 (0.238)	5.49/2.41	3.08	[74]
14	z = 1			620 (0.234)	5.46/2.39	3.07	
	z = 3			620 (0.21)	5.49/2.47	3.02	
Ir-15	z = 0.05	357		421	5.52/–		[75]
	z = 2	357		453, 642	5.51/–		
	z = 4	357		468, 644	5.52/–		
	z = 5	359		473, 644	5.55/–		
Ir-16	y = 0.01	353		562, 594 (0.073)			[76]
	y = 0.03	355		563, 594 (0.08)			
	y = 0.05	360		563, 594 (0.079)			
Ir-17		372		426, 555, 592 (0.09)			[76]
Ir-18a		330		420, 520 (0.33)			[77]
Ir-18b		330		420, 580 (0.20)			[77]
Ir-18c		290		420, 520 (0.29)			[77]
Ir-19	Without pyridine unit	256, 306		531 (0.62)	5.24/2.04	3.20	[77]
	With pyridine unit	256, 306		532 (0.81)	5.33/2.12	3.21	
Ir-21	y = 4	346		595 (0.43)	5.38/2.29	3.09	[80]
	y = 10	348		595 (0.41)	5.35/2.25	3.10	
Ir-22	y = 2	317, 371		595 (0.42)	5.69/2.66	3.03	[81]
	y = 4	317, 371		595 (0.54)	5.71/2.68	3.03	
	y = 10	317, 371		595 (0.54)	5.70/2.67	3.03	
Ir-23a	x = 0.005	360		436, 455, 630 (0.196)			[82]
	x = 0.01			436, 455, 630			
	x = 0.015			436, 455, 630			
	x = 0.02			455, 630			
	x = 0.05			455, 630			
	x = 0.5			630 (0.043)			
Ir-26a		282, 295, 344, 384, 460	515	517 (0.4)			[85]
Ir-26b		296, 330, 344, 385, 437, 487	554	555 (0.19)			[85]
Ir-26c		282, 295, 332, 345, 407, 455, 511	606	609 (0.05)			[85]
Ir-27a		282, 384, 461	515	522 (0.29)			[85]
Ir-27b		290, 310, 325, 385, 438, 488	555	556 (0.22)			[85]
Ir-27c		273, 293, 329, 411, 454, 503	606	612 (0.07)			[85]

[a] Film PL quantum yields were shown in parentheses.
[b] Minus sign is omitted for clarity.
[c] Weak emission.

to the elongation of the conjugated 2-phenylpyridine (ppy) ligands during the polymerization. Similar observation was shown in **Ir-3**, which emits light at ca. 610 nm [65].

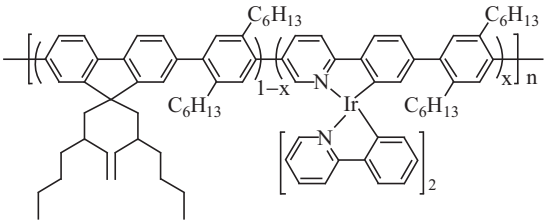

Ir-1 x = 0.02, 0.05, 0.1

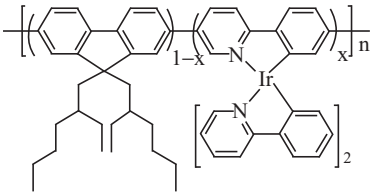

Ir-2

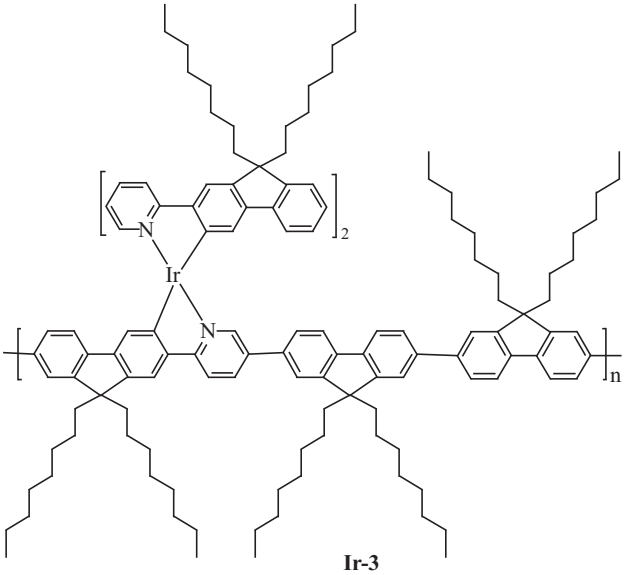

Ir-3

In addition, Ir complexes with different ancillary ligands can also be introduced into the polymer backbone by monobrominated Ir monomers at the 5-position of pyridine in the C^N ligand. Orange-emitting polymers **Ir-4** were reported [66] and their absorption traits are dominated by the poly(fluorene-carbazole) backbones ($\lambda_{max} \sim 350$ nm) but when the Ir content increases (**Ir-4a**: $x = 10$; **Ir-4b**: $x = 10, 20$), a weak triplet MLCT absorption at 480 nm becomes observable. Higher HOMO levels of these copolymers were detected with increasing x value. Unlike the absorption spectra, their PL are dominated by the emission of Ir complex even when its content is low. Only a weak fluorescence emission was observed at 420 nm from the polymer backbone. The film PL emission from Ir complexes displays a slight red-shift with increasing content of Ir complex from 575 nm ($x = 1$) to 585 nm ($x = 10$) in **Ir-4b**. In contrast, no significant red shift in emission wavelength can be observed for **Ir-4b**. The EL from these polymers is more efficient than that from the corresponding blends (i.e. polyfluorene doped with Ir complexes), which demonstrates that these polymers would form a fascinating class of materials through further structural modification. For the complexes bearing acetylacetonate (acac) ligand, the conjugation of polymer backbone is interrupted. Blue-shifted PL was observed in the overall emission of copolymers, although Ir complexes with acac would normally give more red-shifted PL peak.

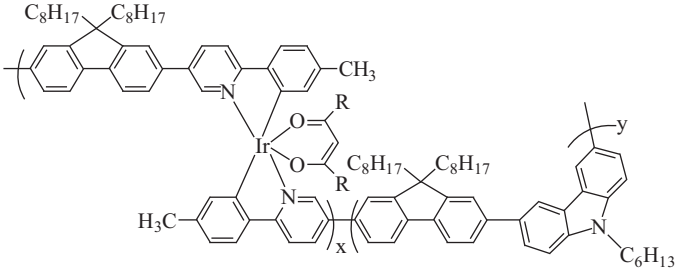

Ir-4 R = CH_3 **a** x = 1, 2, 5, 10

$C(CH_3)_3$ **b** x = 1, 4, 10, 20

Lin et al. reported terpolymers **Ir-5** involving benzimidazole-based Ir complexes with different monomer molar feed ratio [67]. Intense π–π^* absorption of polymer backbone and benzimidazole was observed in the range of 343–382 nm. Since the 3,6-carbazole linkage interrupts the delocalization of π-electrons along the polymer backbone, the absorption bands are shifted to shorter wavelengths as the content of carbazole fragment in polymers **Ir-5a** to **Ir-5d** is increased as compared with **Ir-5e** to **Ir-5h**. Weak MLCT absorption bands appear at 400–500 nm. The authors

found that energy transfer from the polymer backbone to the Ir unit was very inefficient in the dilute solution either intramolecularly or intermolecularly, so that only characteristic π–π^* transition was observed upon photoexcitation. However, phosphorescence emission of the polymer from the Ir units is more obvious in the solid film, especially for a higher concentration (10 and 20 mol%) of Ir units, which indicates the presence of energy transfer from π–π^* transitions to MLCT bands. The efficiency of the energy transfer appears to be higher as the carbazole ratio in the polymer backbone is increased (i.e. **Ir-5f** to **Ir-5h** are more efficient than **Ir-5b** to **Ir-5d**). In such case, more blue residual emissions are apparent in the PL spectra of **Ir-5b** to **Ir-5d**. The Ir content in the copolymer also affects their quantum efficiencies, which decrease as the content of the Ir units is increased due to a greater tendency of triplet-triplet annihilation at a higher Ir concentration. Increasing the proportion of carbazole units also increases the Φ_{PL} of the copolymers.

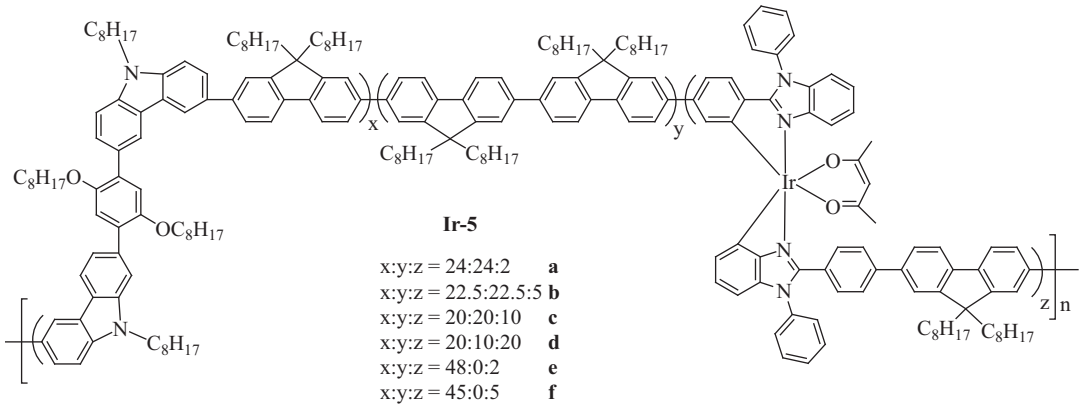

Ir-5

x:y:z = 24:24:2 **a**
x:y:z = 22.5:22.5:5 **b**
x:y:z = 20:20:10 **c**
x:y:z = 20:10:20 **d**
x:y:z = 48:0:2 **e**
x:y:z = 45:0:5 **f**
x:y:z = 40:0:10 **g**
x:y:z = 30:0:20 **h**

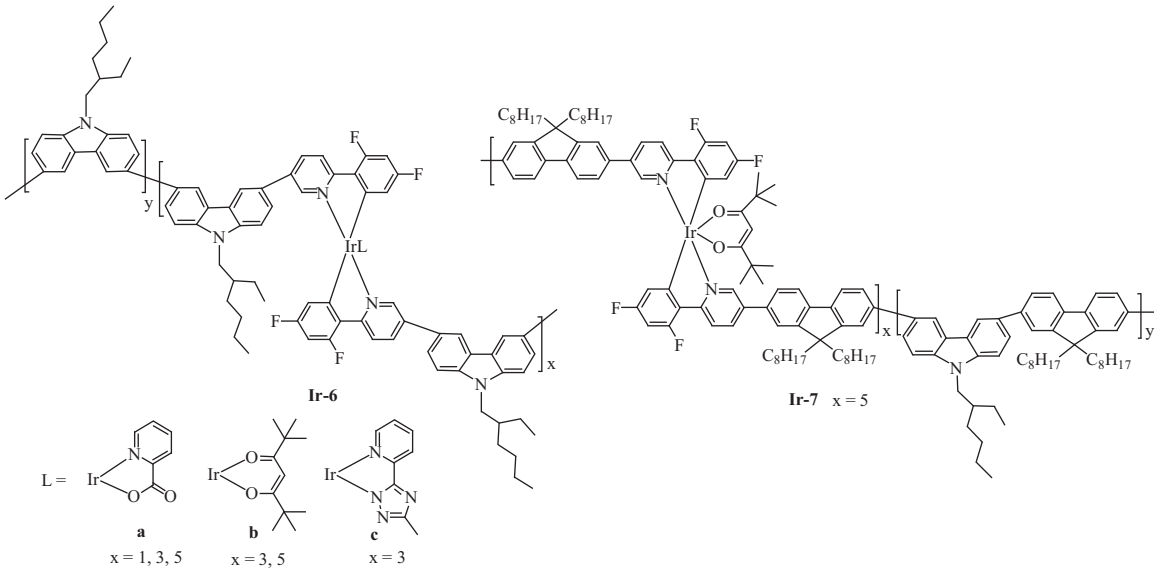

Ir-6

L = **a** x = 1, 3, 5; **b** x = 3, 5; **c** x = 3

Ir-7 x = 5

Compared with orange- or red-emitting polymers, only few green-light-emitting phosphorescent polymers are known for main chain type conjugated polymers. Polymers based on 3,6-carbazole exhibit a wide bandgap and can be used as a host for greenish-blue light-emitting Ir complexes. Yang et al. introduced greenish-blue light-emitting Ir complexes with difluoro-substituted phenylpyridine as C^N ligand and different ancillary ligands into the polymer backbone based on 3,6-carbazole **Ir-6** [68]. They found that the ancillary ligand on the Ir complex would have a clear effect on the luminescence properties and device performance. As the content of Ir increases, a red-shift of absorption peaks was observed in the copolymers (**Ir-6**) with picolinate as the ancillary ligand and a new absorption peak appeared at 420 nm. The MLCT absorption is most red-shifted in copolymers with 3,5-heptanedione ligand. Due to the extended ligand structure (i.e. longer conjugation length) of the Ir complex unit in carbazole-fluorene copolymer **Ir-7**, the PL emission is red-shifted by 30 nm as compared to **Ir-6**. The overall PL efficiency of **Ir-6** (up to 62%) is higher than **Ir-7** (9%), which indicates that 3,6-carbazole is a suitable host for greenish-blue Ir guest. The copolymer with 2,2,6,6-tetramethyl-3,5-heptanedione as an ancillary ligand of the Ir complex has a better luminous performance. The best yellowish green-emitting device was achieved for **Ir-6b** with the maximal LE of 4.4 cd A^{-1} and a luminance of 453 mA cm^{-2} at a current density of 10.3 mA cm^{-2} while the device based on **Ir-7** showed a much poorer performance.

White light emission of a polymer can be realized through the introduction of blue, green and red emissive components into the polymer main chain. For **Ir-8** and **Ir-9** [69,70], white light can be obtained through the simultaneous emission of three primary colors by adjusting the contents of these components. Here, fluorene, benzothiadiazole and Ir complex serve as the blue, green and red emissive species, respectively. The only difference of these two polymers is the replacement of 2-phenylthiophene by isoquinoline as the C^N chelating ligand, and the emission wavelength of red emitter is blue-shifted from 660 to 625 nm. In both cases, by increasing the content of benzothiadiazole, the intensity of red

emission is also enhanced as it provides a bridge to allow a more efficient energy transfer from the fluorene segment to the Ir complex in the PL excitation process. The WPLED device made from **Ir-8** with 0.1 mol.% of Ir complex and 0.03 mol.% of benzothiadiazole shows a maximum EQE of 3.7% and a maximum LE of 3.9 cd A^{-1} at a current density of 1.6 mA cm^{-2} with the CIE coordinates of (0.33, 0.34). The WPLED device fabricated from **Ir-9** with 0.075 mol.% of Ir complex and 0.03 mol.% of benzothiadiazole shows a higher peak luminous efficiency of 5.3 cd A^{-1}, a maximum luminance of 9900 cd cm^{-2} at a current density of 453 mA cm^{-2} and CIE coordinates of (0.32, 0.34).

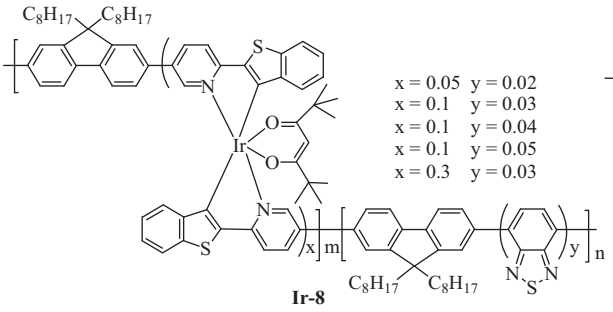

Ir-8

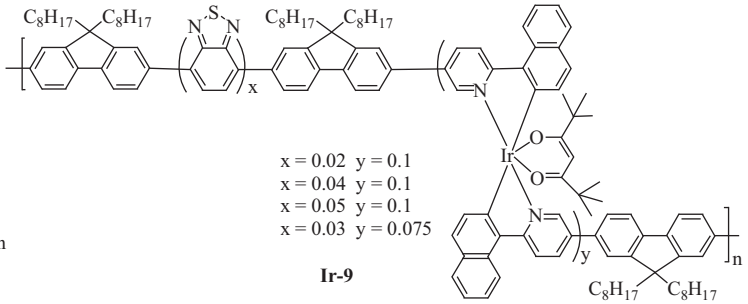

Ir-9

Cationic Ir complexes can also be introduced into a conjugated polymer main chain by using a N^N ligand. Huang and co-workers designed and synthesized a series of polyfluorene derivatives with cationic red-light-emitting Ir complexes in the polymer backbones through a Suzuki polycondensation reaction (**Ir-10** to **Ir-13**) [71–73]. Saturated red-light emission can be realized by choosing appropriate C^N and N^N ligands. Like the neutral polymers, absorption of cationic polymers is dominated by the polymer backbone. An almost complete energy transfer from the host to the Ir complex guest was achieved in the solid state even at a low feed ratio of the complex. In order to further improve the optoelectronic properties of this series of interesting materials, the carbazole unit was also introduced into the backbone (**Ir-13**) or the side chain (**Ir-11**) of polymers. The introduction of a carbazole unit has a strong impact on the hole injection and charge attraction ability of the polymers as well as the host–guest energy transfer efficiency. The oxidation potential is slightly lowered by about 0.08 V in **Ir-11** as compared to **Ir-10**.

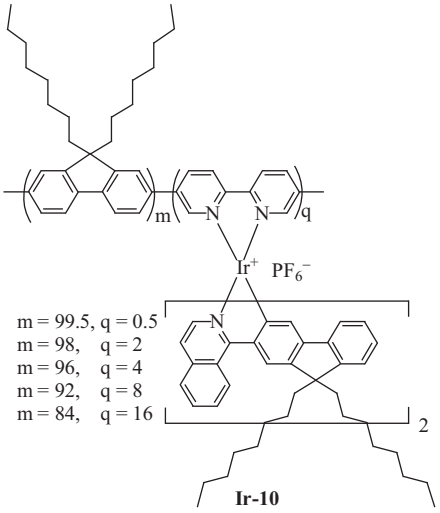

Ir-10

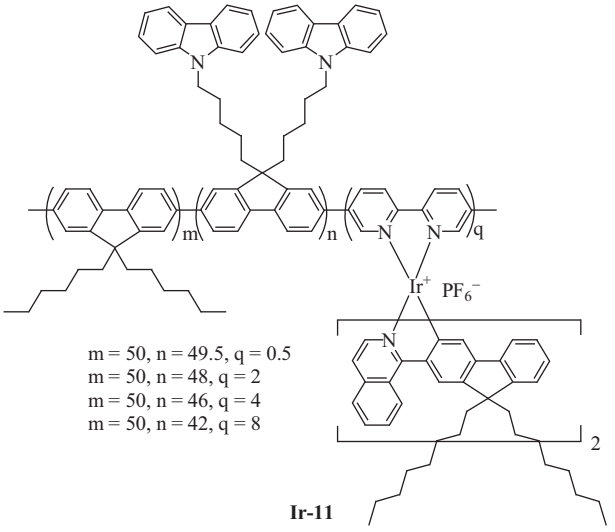

Ir-11

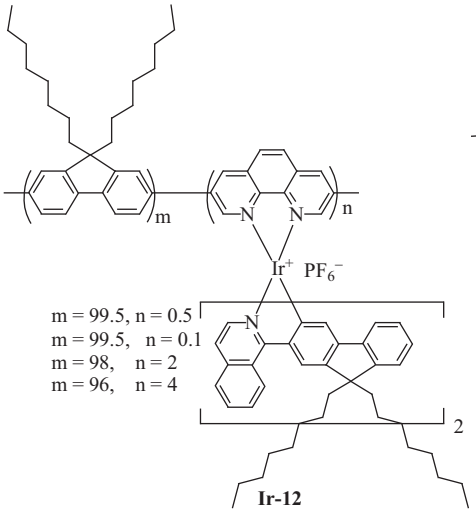

Ir-12

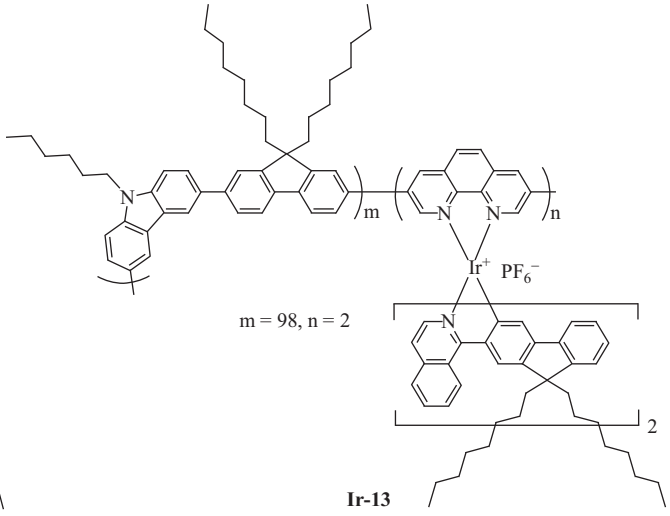

Ir-13

5.1.2. Conjugated polymers with O^O ligand of neutral Ir complexes on the main chain

Conjugated polymer with Ir complexes on the main chain **Ir-14** to **Ir-16** can also be realized by introducing a β-diketone O^O-type ligand of neutral Ir complexes into the polymer main chain through a Suzuki polycondensation reaction. Saturated red-emitting PLEDs were reported by using **Ir-14** [74] and **Ir-15** [75] as the active layers. Since the π-conjugation length appears to be disturbed by an ancillary unit in the polymer chain, it would lead to a shortening of the effective conjugation length of the main chain using O^O ligand as compared to those of N^N and C^N. The emission of this type of Ir polymers only shows slightly red-shifted peak from their corresponding organic backbone. This approach provides an additional advantage to control the emission wavelength of the chelating copolymers. The EL spectra of **Ir-14** show exclusive triplet emission even with the feed ratio of Ir complex as low as 0.5 mol.%. This indicates the complete quenching of the host backbone emission at 420 nm with a lower content of Ir complex. For the single-layer devices of the configuration ITO/PEDOT:PSS/copolymer/Ba/Al, the efficiencies increased from 0.05 to 0.24% when the feed ratio of Ir complex was changed from 0.5 to 3 mol.%. In addition, Ir complexes can also be introduced into the terminal group of the PF main chain by a β-diketonate ligand in **Ir-17** [76]. The absorption peak of **Ir-16** (λ_{em} = 353–360 nm) experiences a blue-shift of over 10 nm compared with **Ir-17** (λ_{em} = 372 nm) since the linear conjugated system of polyfluorene is interrupted by the 3,6-linked carbazole unit in the backbone. In contrast to **Ir-16**, the emission of backbone unit at 420 nm is more intense than the emission at 555 nm and 592 nm from the Ir complex in **Ir-17**. This may be attributed to the very low loading of Ir complex in **Ir-17**. The EL device using Ir core-containing end-capped polymers as the emitting layer displays significantly higher EQEs than those based on a copolymer with the Ir complex embedded in the main chain, although the content of the Ir complex in the former is much lower than that in the latter. This may be mainly attributed to the fact that the end-capping polymer suffers from less triplet energy back-transfer from the Ir complex to the polymer backbone. Therefore, this represents an important improvement in the design of electroluminescent polymers.

In addition to the linear main-chain Ir polymers, the highly branched polymers **Ir-18** and **Ir-19** can depress the aggregation and excimer formation, so that the materials tend to form amorphous films with good quality, and consequently the light-emitting efficiencies can be improved. The hyperbranched copolymers **Ir-18b** emit green light with λ_{max} = 520 nm and the linear-type of its similar copolymer is yellow-emitting with λ_{max} = 580 nm [77]. **Ir-18a** and **Ir-18c** exhibit similar optical profiles to each other but **Ir-18b** shows red-shifted emission as compared to them. A red shift of about 20 nm was observed in **Ir-19** (λ_{em} = 531–532 nm versus the parent Ir(ppy)$_3$ with λ_{em} = 510 nm), which is ascribed to the longer extended conjugation in the ligand from the copolymerized carbazole unit [78].

The HOMO energy level of **Ir-19a** is ∼−5.24 eV, but it decreased to −5.33 eV for **Ir-19b** with the addition of a pyridyl linker. While the LUMO value of **Ir-19b** also dropped to −2.12 eV, a further decrease of both frontier orbital levels would be anticipated if more 2,6-pyridine rings are introduced because the incorporation of the electron-deficient pyridine moiety into the polymer branches would evidently lower the electron injection barrier. In this series of green-emitting hyperbranched polymers, the best performance was achieved from **Ir-19b** (x = 10), in which 10 mol.% content of pyridine unit was incorporated into the branched host segments, giving a peak EQE of 13.3%, peak LE of 30.1 cd A^{-1} and power efficiency (PE) of 16.6 lm W^{-1} at 2.4 mA cm^{-2} and 5.7 V, while the peak luminance reaches 82059 cd m^{-2}. These figures are four times more efficient or brighter than those of the device fabricated from pyridine-free **Ir-19a** at the same feed ratio. Therefore, the addition of pyridine into the polymer chain would benefit the PLED performance.

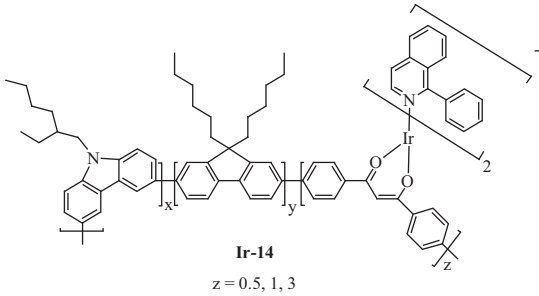

Ir-14

z = 0.5, 1, 3

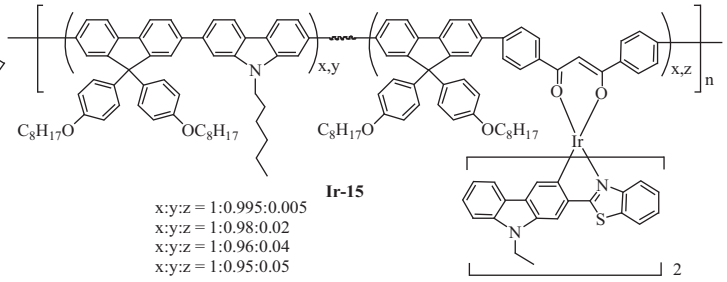

Ir-15

x:y:z = 1:0.995:0.005
x:y:z = 1:0.98:0.02
x:y:z = 1:0.96:0.04
x:y:z = 1:0.95:0.05

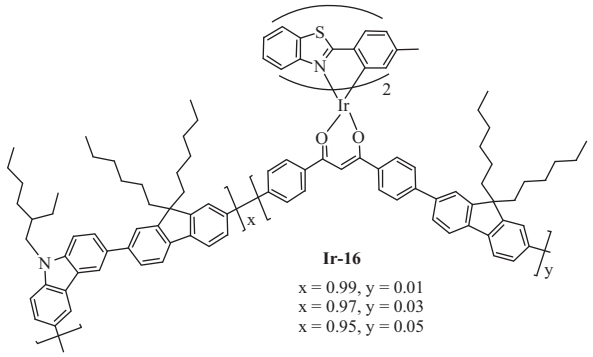

Ir-16

x = 0.99, y = 0.01
x = 0.97, y = 0.03
x = 0.95, y = 0.05

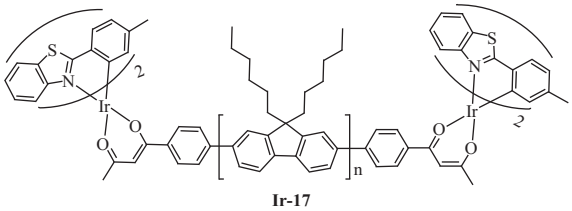

Ir-17

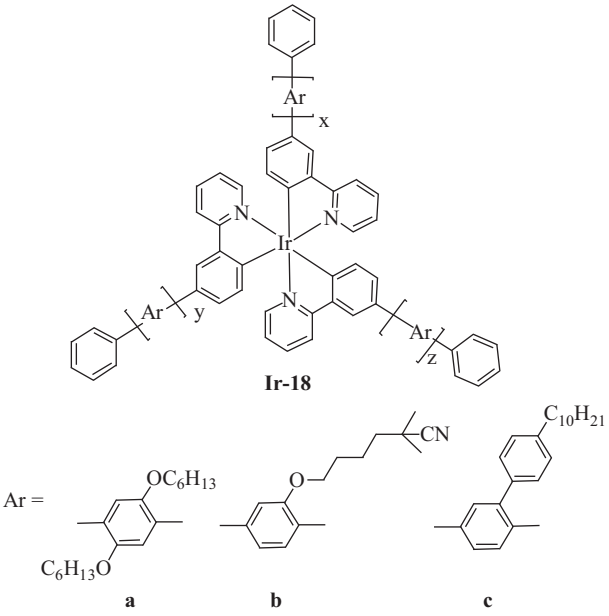

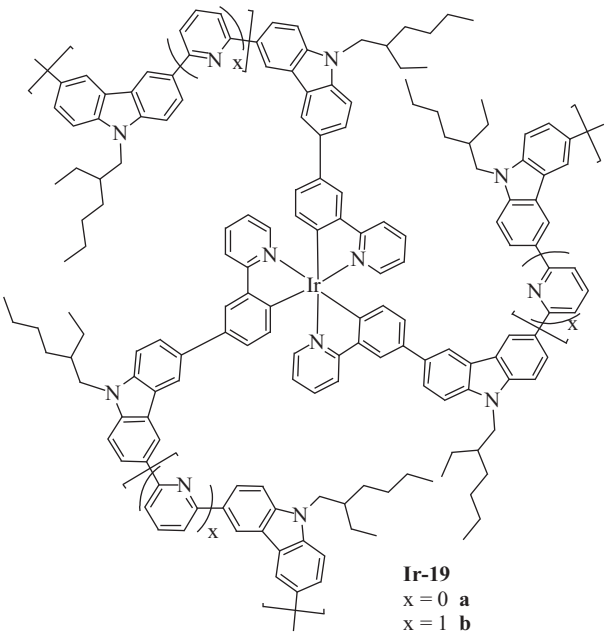

5.2. Polymers with Ir(III) complexes in the side chain

5.2.1. Conjugated polymers with Ir(III) complexes in the side chain

Conjugated polymers with Ir complexes in the side-chain can be realized by grafting the O^O, C^N, or N^N ligand onto the C-9 position of fluorene or the *N*-position of carbazole through a spacer such as the long alkyl chain. Polyfluorenes or fluorene-*co*-carbazole copolymers often act as the polymer main chains. Up to now, highly efficient red-emitting and white-emitting conjugated polymers with Ir complexes in the side-chain have been realized. The pioneering work of conjugated polymers with Ir complexes was first reported by Chen et al. through grafting polyfluorene with green- and red-emitting cyclometalated Ir complexes at the C-9 position of fluorene (**Ir-20**) [79]. In addition, carbazole units were also introduced into the side-chain of polyfluorene as the charge-transport moiety and a source for green emission by forming an electroplex within the polyfluorene main chain. PL spectra of the polymers without the carbazole moiety show blue emission from the main chains and additional red emission from the Ir complexes (except for the case when the red-emitting Ir content is too low (e.g. **Ir-20a**, $m = 0.1$; $n = 99.9$). If an additional 0.5 mol.% green-emitting Ir complex in the feed is incorporated (e.g. **Ir-20d**, $m = 0.1$; $n = 99.4$; $p = 0.5$), a weak red emission appears. Both the energy transfer from the main chain and the formed electroplex to the red-emitting Ir complex can significantly enhance the device performance. The green-emitting Ir complex in the copolymer may also behave as a bridge to facilitate energy transfer from the main-chain to the red-emitting Ir complex through a sequential energy transfer process. The device from **Ir-20f** showed an EQE of 1.59% and a LE of 2.8 cd A^{-1} at 7.0 V with a luminance of 65 cd m^{-2} and a peak emission at 610 nm. Also, a series of orange- and red-emitting copolymers (**Ir-21** to **Ir-23**) were reported [80–82]. Their colors are tuned by suitable choice of cyclometalating ligands on the Ir complex. The polymer backbone only gives absorption bands between 300 and 400 nm and no Ir-based transition bands beyond 450 nm were detected if the Ir content is low. Charged copolymers **Ir-21** to **Ir-22** with isoquinoline gave red colors (595 nm) from PLEDs and the λ_{em} is rather independent of the copolymer compositions or monomer types. The HOMO and LUMO levels of these polymers showed no essential differences from those in their corresponding macroligands. This further indicates that attachment of the Ir complexes in the side chain did not alter the backbone and conjugation length of the host polymers. Red emission was also achieved by using **Ir-23a** with 2,4-diphenylquinoline as the chelating ligand, but if fluorinated ligand was used instead as shown for **Ir-23b** and **Ir-23c**, the emission color was blue-shifted, emitting in the orange-red and orange region, respectively. By combining with the blue emission from polyfluorene backbone, white PLEDs can be fabricated [82].

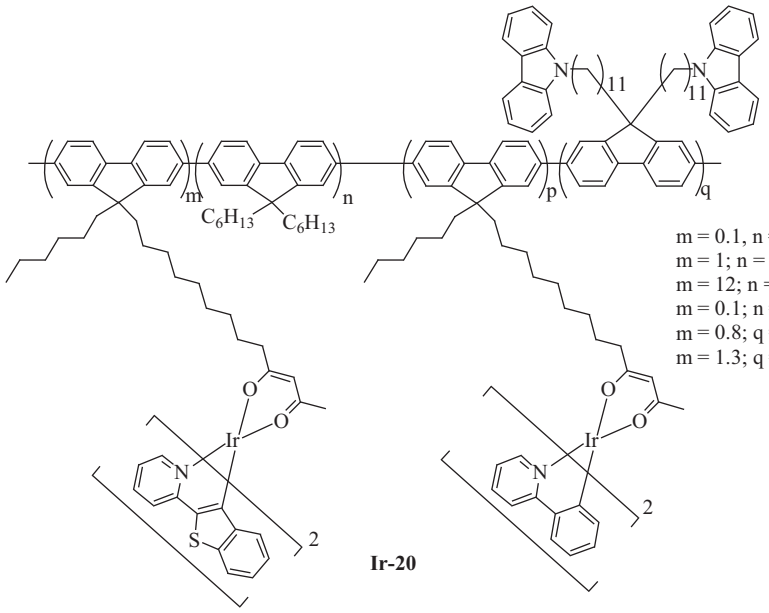

m = 0.1, n = 99.9 **a**
m = 1; n = 99 **b**
m = 12; n = 88 **c**
m = 0.1; n = 99.4; p = 0.5 **d**
m = 0.8; q = 99.2 **e**
m = 1.3; q = 98.7 **f**

Ir-20

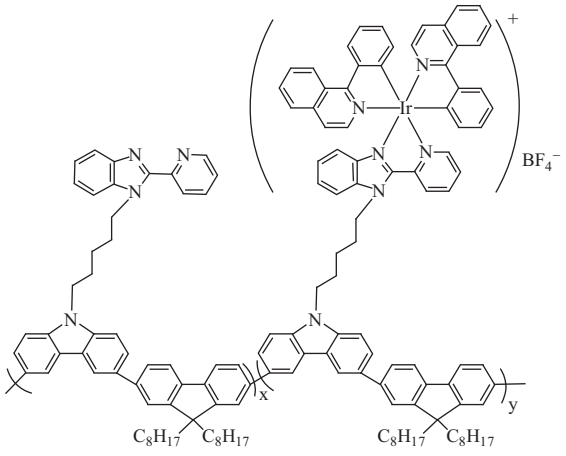

Ir-21
y = 4, 10

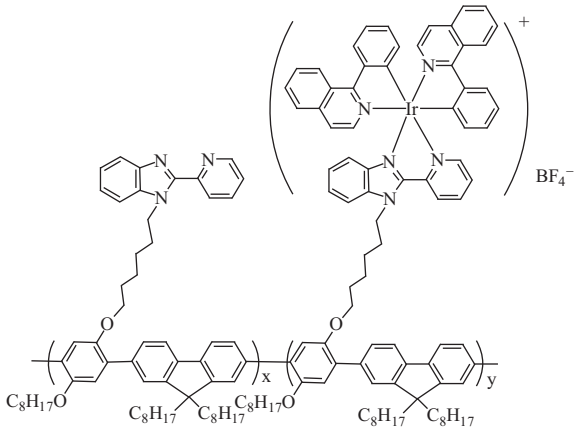

Ir-22
y = 2, 4, 10

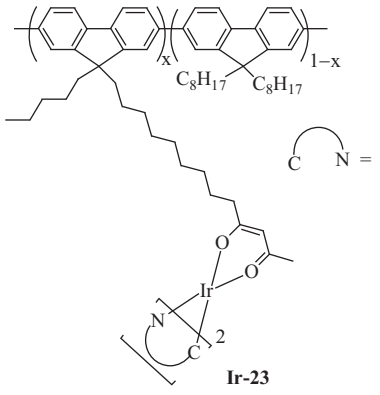

Ir-23

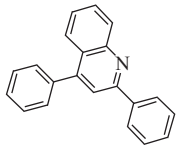

a

x = 0.005
x = 0.01
x = 0.015
x = 0.02
x = 0.05
x = 0.5

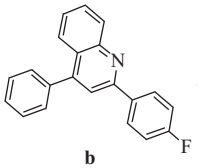

b

x = 0.005
x = 0.01
x = 0.02

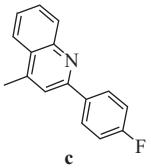

c

x = 0.01
x = 0.02
x = 0.03

Highly efficient white PLEDs from a single polymer (**Ir-24**) was also reported by combination of a fluorene-based blue emitter of large E_g, a green benzothiadiazole-derived emitter and an isoquinoline-based Ir complex as the triplet red-light-emitting species [83].

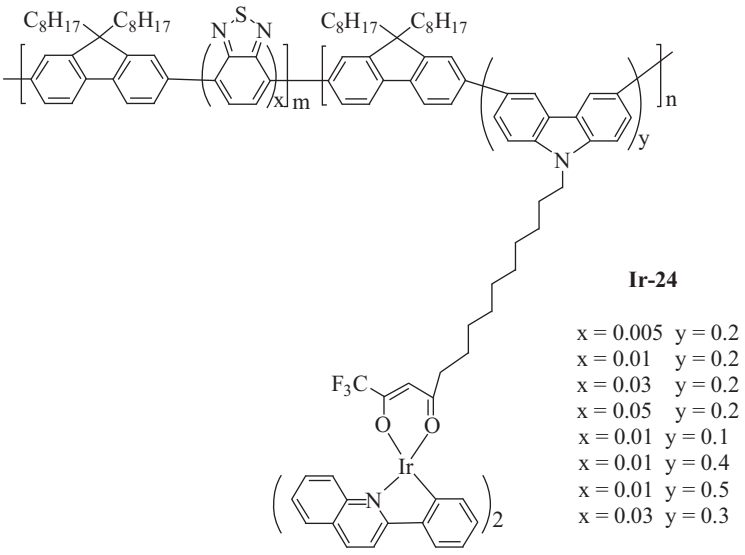

Ir-24

x = 0.005 y = 0.2
x = 0.01 y = 0.2
x = 0.03 y = 0.2
x = 0.05 y = 0.2
x = 0.01 y = 0.1
x = 0.01 y = 0.4
x = 0.01 y = 0.5
x = 0.03 y = 0.3

The introduction of both electron- and hole-transporting units into the C-9 position of fluorene as side-chains is a very effective method to improve the device performance. Based on this design concept, Neher and co-workers have introduced electron-transporting oxadiazole and hole-transporting triphenylamine into the C-9 position of fluorene and synthesized a series of electrophosphorescent polymers **Ir-25** [84]. A red-emitting Ir complex was attached to the C-9 position of fluorene through a picolinate C^O-type ligand. During the fabrication of PLEDs, the incorporation of a hole-transporting/electron-blocking interfacial layer poly(9,9-dioctylfluorene-*co*-bis-*N*,*N*-(4-butylphenyl)-bis-*N*,*N*-phenyl-1,4-phenylenediamine) (PFB) and utilization of an efficient electron-injection cathode CsF/Ca/Al improved the device performance and led to saturated red-emitting polymer electrophosphorescent devices with a peak LE and PE of 9.3 cd A^{-1} and 10.5 lm W^{-1}, respectively. The excellent performance of the devices was attributed to the well-defined carrier recombination zone.

5.2.2. Non-conjugated polymers with Ir(III) complexes in the side chain

For the non-conjugated polymer hosts, PVK and its derivatives are often employed because of their high energy blue emissive singlet excited state, favorable film-forming properties, good durability at high temperature and excellent hole mobility. For this type of polymers, their UV–vis absorption spectra display characteristic π–π^* transitions originating from the ligands of the Ir complexes and other moieties attached to the PVK chain and a weak MLCT absorption from the Ir complexes. The emission maxima of the copolymers are similar to those of the corresponding small-molecule Ir complexes. Therefore, the polymer backbones do not affect the absorption and emission properties of the tethered metal complexes. Usually, the obtained Φ_{PL} of different polymers are comparable to their small-molecule analogues. Taking **Ir-26** and **Ir-27** as examples [85], the copolymers retained the optical properties associated with their small-molecule analogues both in solution and solid states. They emit at 515, 554 and 606 nm for **Ir-26a**, **Ir-26b** and **Ir-26c**, respectively, and the situation is the same for **Ir-27**, so copolymers with or without carbazole groups have similar optical properties. Similar lifetimes were also recorded in both series, indicating that there is no emission quenching related to carbazole units.

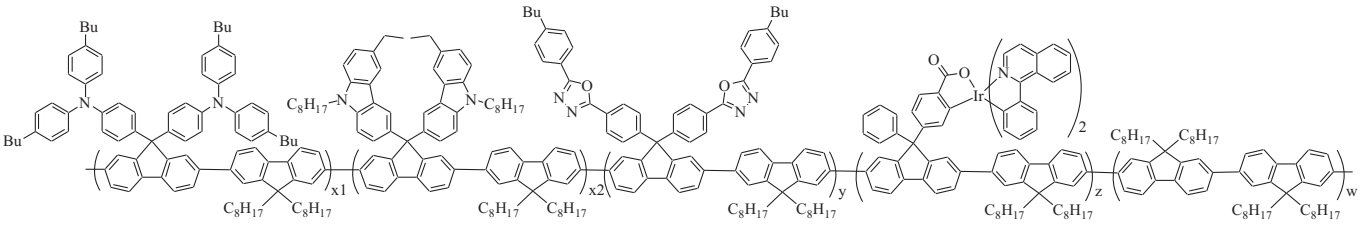

Ir-25

x1 = y = 0.225n, z = 0.05n, x2 = w = 0
x1 = 0.10n, y = 0.225n, z = 0.05n , w = 0.125n, x2 = 0
x2 = y = 0.225n, z = 0.05n, x1 = w = 0
x2 = 0.10, y = 0.25n, z = 0.05, w = 0.10n, x1 = 0

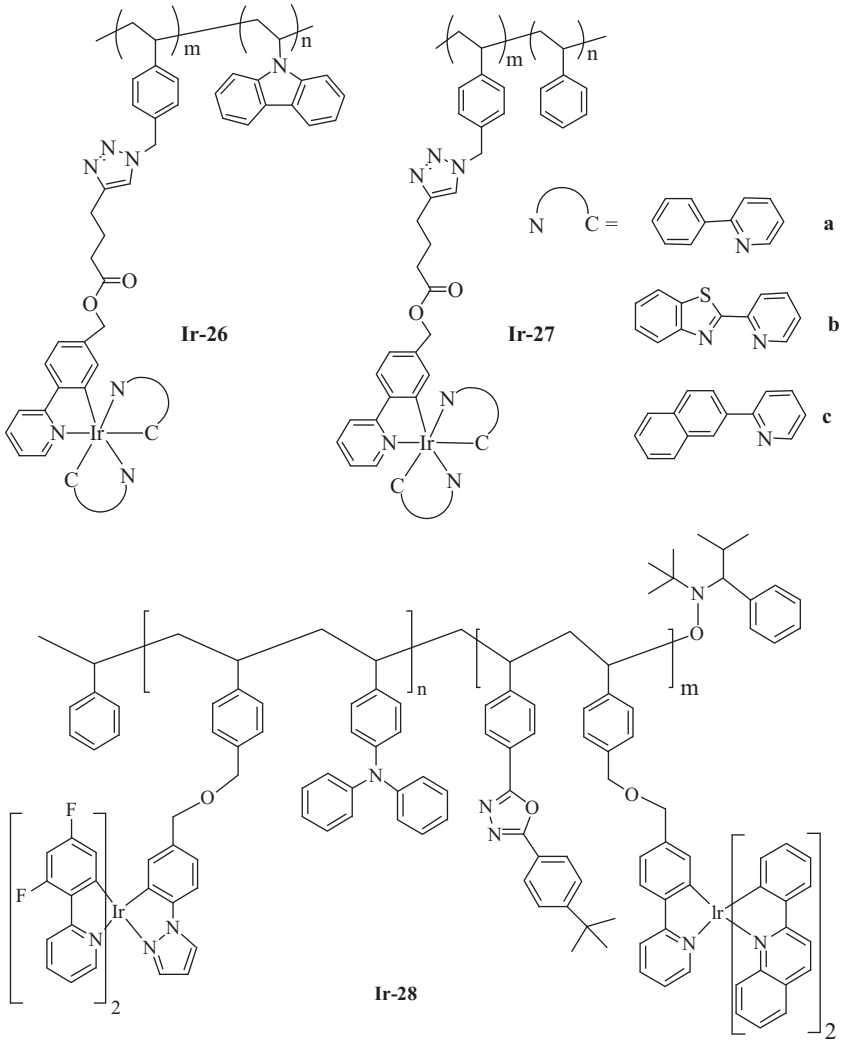

For the realization of white PLEDs, more than one phosphorescent emitter can be present in a single polymer. As a result, the EL color may be affected by the energy transfer between emitters. Block copolymers **Ir-28** allow hierarchical supramolecular control over the spatial location of their functional components as well as various nanometer-scale blocks [86]. Therefore, these can have the unique potential to spontaneously achieve phosphorescent emitter isolation through self-assembly and suppressing the occurrence of energy transfer. Fréchet and co-workers synthesized a bichromophoric block copolymer **Ir-28** through living radical polymerization. The first block was synthesized by a random copolymerization of triarylamine with $[Ir(dfppy)_2(tpzs)]$ (dfppy = 2-(2,4-difluorophenyl)pyridine; tpzs = 1-*p*-tolylpyrazole), followed by addition of the second block in a random copolymerization of oxadiazole with $[Ir(pq)_2(tpys)]$ $[Ir(dfppy)_2(tpzs)]$ and $[Ir(pq)_2(tpys)]$ show phosphorescence emissions in the green/blue and orange/red regions of the visible spectrum, respectively. The authors have explored the use of these copolymers as the single active layer in PLED devices to investigate the fundamental effect of both molecular weight (MW) and the ratio of blue to red Ir complexes on the overall emission color and device performance. It is clear that increasing the MW of polymer results in lower emission intensity from the red chromophore $[Ir(pq)_2(tpys)]$. In particular, a significant decrease in red emission with a concomitant increase in blue emission is seen when the MW is increased from 3×10^4 Da to 7×10^4 Da while keeping the blue to red ratio constant at 10:0.5. An increase in MW from 7×10^4 Da to 10^5 Da leads to a further decrease in red emission intensity. It is clear that the use of larger blocks enables a more balanced dual emission at higher red dye content. They also found that nanophase separated morphology can be obtained by increasing the block size in the copolymers, which affords the site-isolation of chromophores necessary for suppressed energy transfer and improved device performance.

6. Platinum(II)-containing polymers

The propensity of heavy platinum(II) ion to allow mixing of singlet and triplet excited states, high phosphorescence yields and relatively long emission lifetimes of their compounds all would render the Pt-containing materials attractive in optoelectronic devices with different degrees of contributions. Two main types of polymer are commonly found, one consisting of linear rod-like Pt polymetallaynes and the other containing cycloplatinated moieties.

6.1. Platinum(II)-containing metallopolyynes

In the area of synthetic Pt-containing polymers, rigid-rod Pt(II) acetylide polymers have spurred tremendous global interest. A large series of soluble Pt(II) derivatives incorporating various conjugated ring systems have been reported with diverse photophysics and materials properties, that are applicable in various domains of

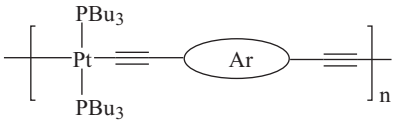

Fig. 4. The general structure of polyplatinynes.

molecular optoelectronic applications. The basic structure of polyplatinynes is shown in Fig. 4. There are several reported approaches to tune the optical properties of this kind of polymers and the simplest way is to enhance the π-conjugation in the bridging ligands. Due to the fact that the delocalization of electrons can be maintained along the polymer chain by the π-conjugation between the orbitals of Pt and the ligands, the degree of π-electron delocalization of the central bridge (Ar) would have a profound effect on the PL properties. Another way is to localize the electron density or by partially destroying ligand aromaticity so that non-conjugated or weakly conjugated system can be obtained. This type of polymer generally has high-energy triplets to avoid competition with non-radiative decay. Functionalization on different organic spacers and a control of the D–A interactions between the bridging units can also be used to adjust the electronic and morphological properties. Therefore, by choosing different types of organic spacers, these metallopolymers can display a wide range of colors, E_g as well as fluorescent and phosphorescent emissions in solution and solid states as illustrated in Figs. 5–8 and Table 4. Clearly, it is evident that the absorption and PL peaks can scan a wide color range in the full visible spectrum for these polymers.

Generally speaking, the absorption features of Pt polyynes are mainly assigned to the ^{1}IL π–π* transitions of the metal-acetylide conjugated chromophore. With reference to the absorption maximum for the ligand, there is a typical bathochromic shift of the position of the lowest energy absorption band after metal fragments are introduced. Polymer **Pt-1a** with the phenylene spacer absorbs at 380 nm [87–89], and π-conjugation is enhanced by doubling the number of C≡C units on each side of the phenylene ring in **Pt-1b**, leading to a red shift in absorption and phosphorescence wavelength from 380 to 396 nm [90,91]. With an increase of the

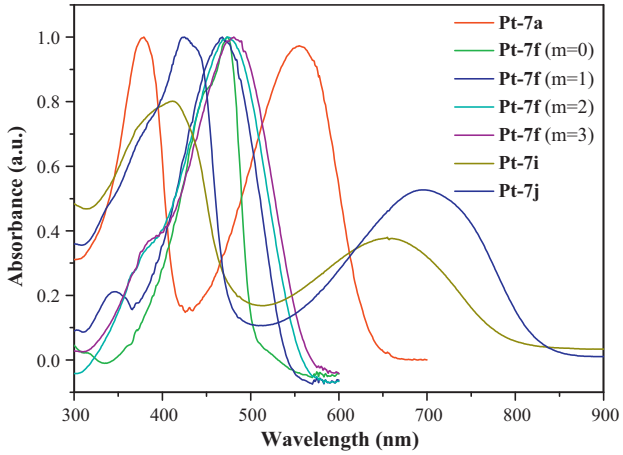

Fig. 6. Absorption spectra of polyplatinynes spanning a full color spectrum (see Ref. [114,116,118]).

oligothiophene length, the E_g value of **Pt-2** series decreases from **Pt-2a** to **Pt-2c** and the emission features are shifted to the lower energy side because of an increased delocalization of π-electrons along the polymer chain [92]. But the reduction in E_g from **Pt-2a** to **Pt-2c** becomes less significant as the number of thienyl rings increases. The relative proportion of Pt to the organic spacer causes the energy of the triplet emission to show a red shift along the series with a rapid drop of triplet emission intensity (i.e. triplet energy of **Pt-2a** > **Pt-2b** > **Pt-2c**). The measured singlet–triplet (S_1–T_1) separations lie essentially constant at 0.75–0.80 eV (Fig. 9). A series of oligopyridine-linked Pt(II) polyynes **Pt-3** [93–95] has been reported. From their optical absorption and PL data, conjugation is increased along **Pt-2a** > **Pt-1a** > **Pt-3a** but the intersystem crossing rate is reduced by the electron-rich thiophene ring relative to the phenylene unit, whereas the opposite trend is observed for the electron-deficient pyridine group. Quaternization of the pyridyl nitrogen (**Pt-3b**) leads to a strong bathochromic shift in the absorption spectrum (λ_{max} = 440 nm) (versus **Pt-3a**: λ_{max} = 382 nm) due to improved π-conjugation accompanied by an increase in Φ_{PL}. The

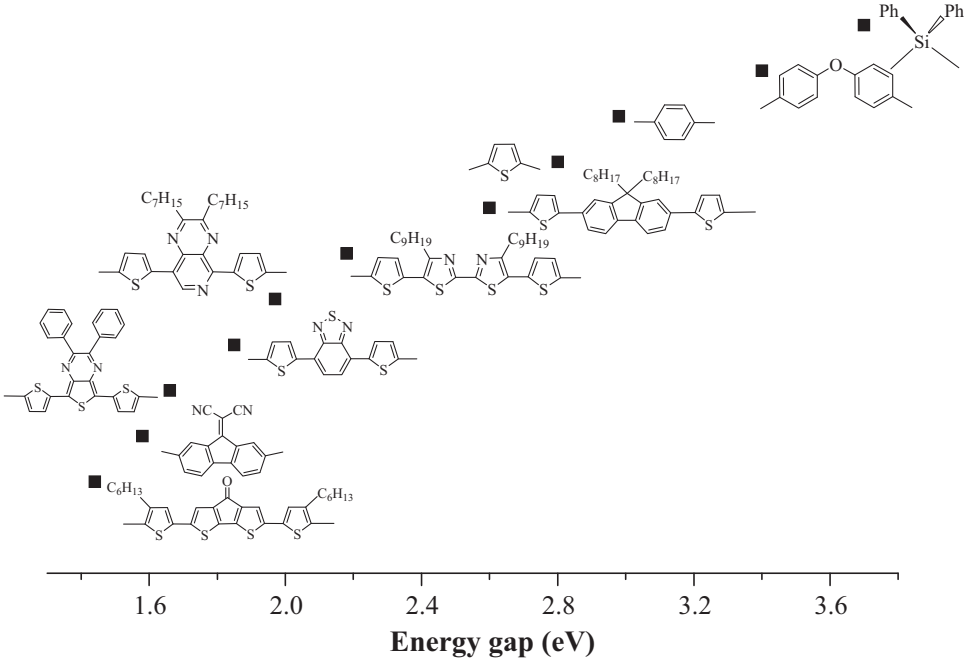

Fig. 5. A wide spectrum of E_g values (in eV) for Pt polyynes with different spacer groups (see Ref. [87,89,92,96,101,105,113,114,116–119]).

Table 4
Photophysical data of Pt(II)-containing polymers.

Polymer	$\lambda_{max,abs(sol)}$ [nm]	$\lambda_{max,abs(film)}$ [nm]	$\lambda_{em,PL(sol)}$ [nm]	$\lambda_{em,PL(film\ or\ frozen)}$ [nm] (<100 K)	HOMO/LUMO[a] [eV]	E_g [eV]	Ref.
Pt-1a	380	380	516	405, 521		2.98	[87,89]
Pt-1b	396			569		2.60	[90,91]
Pt-2a	416	224, 264, 308, 407		435, 605		2.80	[92]
Pt-2b	458	230, 268, 301, 446		508, 742		2.55	[92]
Pt-2c	470	233, 272, 334, 457, 484		544, 810		2.40	[92]
Pt-3a	382	378		387, 523		3.00	[93,94]
Pt-3b	440						[93,94]
Pt-3c		394		426, 569		2.90	[95]
Pt-3d		344		463		3.30	[95]
Pt-3e		344		461		3.30	[95]
Pt-4a	261, 277, 312	261, 278, 314	418, 510[b]	419, 508		3.70	[96]
Pt-4b	303, 355	304, 360	404, 520 394, 513, 575[b]	394, 423, 512, 555, 575		3.10	[96]
Pt-5a	267, 292, 343	266, 291, 337	368, 492	454, 475, 488		3.40	[101]
Pt-5b	269, 296, 352	294, 344	382, 482	484, 510, 522, 537		3.26	[101]
Pt-5c	272, 299, 349	266, 299, 337	382, 474	475, 501, 527		3.28	[101]
Pt-5d	270, 301, 361	268, 301, 350	389, 481	484, 509, 536		3.18	[101]
Pt-6a	307, 399	309, 404	421, 555 432, 552[b]	416, 433, 554, 589, 606		2.92	[102]
Pt-6b	392, 467		588	530		2.17	[103]
Pt-6c	382, 506	503	546 541[b]	546		2.10	[104]
Pt-6d	303, 348, 393, 660		421, 680, 698			1.58	[105]
Pt-6e	355–382, 437		437			2.10	[106]
Pt-6f	258, 301, 344	261, 304, 347	412, 428 404, 427[b]	403, 426, 462, 497, 511		3.10	[102]
Pt-6g	264, 390		408, 428, 527, 567	414, 436, 524[b], 572		2.95	[107]
Pt-6h	284, 292, 326, 346, 360, 370			395,422, 455, 477, 490, 504, 564[b]			[108]
Pt-6i	324, 348, 370			395,420, 458, 483, 505, 540[b]			[108]
Pt-7a	554		680	704	5.37/3.14	1.85	[116]
Pt-7b	566	592			5.18/3.34	1.84	[121]
Pt-7c	588	610			5.12/3.30	1.82	[121]
Pt-7d	596	611			5.14/3.33	1.81	[121]
Pt-7e	453, 473		496		5.72/3.32	2.40	[109]
Pt-7f							[118]
$m=0$	452, 474		497	508, 536	5.91/3.51	2.40	
$m=1$	345, 468		557		5.82/3.64	2.18	
$m=2$	378, 476		592		5.79/3.69	2.10	
$m=3$	397, 481		603		5.71/3.65	2.06	
Pt-7g							[117]
$m=0$	307, 399				5.88/3.86	2.93	
$m=1$	420, 439				5.85/3.87	2.60	
$m=2$	446, 463				5.79/3.87	2.43	
$m=3$	457				5.73/3.89	2.33	
Pt-7h		506		556, 747		2.25	[112]
Pt-7i	412, 656	419, 681			5.46/3.96	1.50	[114]
Pt-7j	424, 694	424, 714			5.40/3.89	1.47	[114]
Pt-7k	412, 651	415, 674			5.22/3.51	1.54	[113]
Pt-7l	402, 609	407, 622			5.36/3.34	1.66	[113]
Pt-7m	415, 655	415, 674			5.44/3.96	1.50	[115]
Pt-7o	375, 532	380, 543			5.59/3.35	1.97	[113]
Pt-7p	279, 307, 399, 641				5.57/3.88	1.53	[119]
Pt-7q	271, 414, 653				5.44/3.89	1.44	[119]
Pt-8a	335, 610	750 (onset)			5.4/3.5	1.65	[123]
Pt-8b	375, 520	600 (onset)			5.6/3.5	2.1	[123]
Pt-8c	374		585	584, 634			[123]
Pt-8d	374		585	584, 634			[123]
Pt-9a	261, 315, 427, 435, 518, 558, 599		390, 452, 611, 659	398, 413, 452, 471, 498, 530, 606, 662, 723, 803			[125]
Pt-9b	264, 282, 327, 433, 426, 525, 561, 604		396, 446, 616, 662	393, 418, 450, 472, 495, 53, 615, 638, 667, 703, 823			[125]
Pt-9c	302, 466, 678		682, 754	684, 754			[126]
Pt-9d	302, 462, 676		680, 750	685, 770			[126]
Pt-10	229, 260, 287, 379, 400, 446, 465, 487		549, 588	552, 599			[127]
Pt-11	229, 251, 283, 383, 400, 474, 502		577, 625	577, 631			[127]

[a] Minus sign is omitted.
[b] Shoulder peaks.

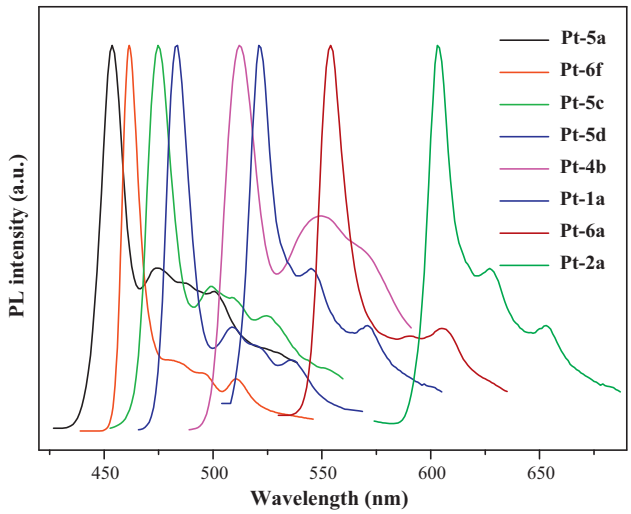

Fig. 7. Phosphorescence spectra of polyplatinynes exhibiting a wide color range (see Ref. [87,89,92,96,101,102]).

change of ligand configuration also affects the optical properties of the resulting polymers. For **Pt-3c**, the inclusion of a second pyridine unit shifts E_g to the red by 0.1 eV relative to **Pt-3a**, but to the blue relative to **Pt-3d** and **Pt-3e**. This agrees with the fact that **Pt-3a** and **Pt-3c** with the alkynyl groups at the 5,5-positions is fully conjugated, whereas in **Pt-3d** and **Pt-3e**, the alkynyl units at the 6,6′- or 6,6″-positions hinders conjugation between the pyridyl rings [94]. Thanks to the reduced conjugation in **Pt-3d** and **Pt-3e**, they possess higher energy for the T_1 states with no fluorescence emission detected at 10 K.

The excited-state transitions can be tuned by localizing the electron density in discrete regions of the molecules or by partially destroying ligand aromaticity. The exploitation of some main group elements in the build up of polymetallaynes has also proliferated the advance of this field. The degree of conjugation becomes significantly poor in the presence of a silyl unit (**Pt-4a**) [96] but this is good for improving the phosphorescence properties as compared to the more conjugated Pt polymers mentioned before. **Pt-4b** also recorded a very high efficiency of triplet emission, with greater than unity ratio of phosphorescence to fluorescence integrated intensities [97–99]. The work was then extended to other polyplatinynes containing oligo(aryleneethynylenesilylene)s and oligo(aryleneethynylenegermylene)s displaying intriguing photophysical traits and trends [100].

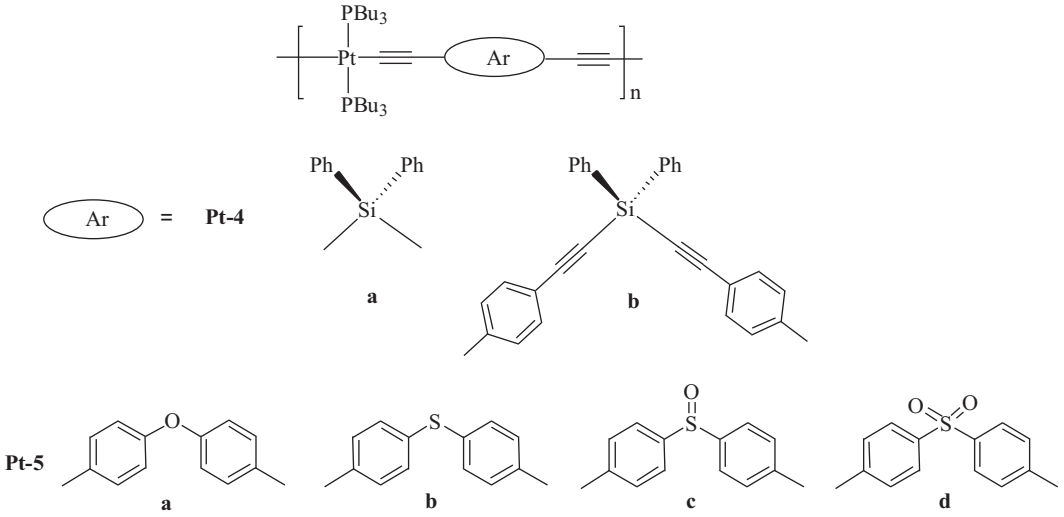

The use of main group 16 segments (**Pt-5**) also greatly enhances the room-temperature phosphorescence as compared to other π-conjugated Pt polymetallaynes. Polymer **Pt-5a**, with the diphenylether linkage, has the most red-shifted emission signal, which exceeds that of the sulfide analogue **Pt-5b** due to the higher degree of conjugation of the more polarizable S over O atoms [101]. However, the change of different main group units does not affect the phosphorescence quantum yields very much.

Functionalization of the 9-position of fluorene can easily adjust the photophysical and electronic properties of the polymers **Pt-6** as well. We should note that the rigid planar biphenyl unit in fluorene ensures a higher degree of conjugation, hence improving the luminescence efficiency of the materials as compared to the *p*-phenylene derivatives. A list of fluorene-based polyplatinynes **Pt-6a** to **Pt-6e** have been investigated and by changing the substituents at the C-9 position of fluorene ring, the optoelectronic properties of these metal-containing polymers can be chemically modified [102–106]. These metalated materials can display a variety of colors and E_g values in the solid state. The E_g follows the order of **Pt-6a** (2.92 eV) > **Pt-6b** (2.17 eV) > **Pt-6c** ~ **Pt-6e** (2.10 eV) > **Pt-6d** (1.58 eV), consistent with the nature of the attached group from the weakly electron-donating alkyl

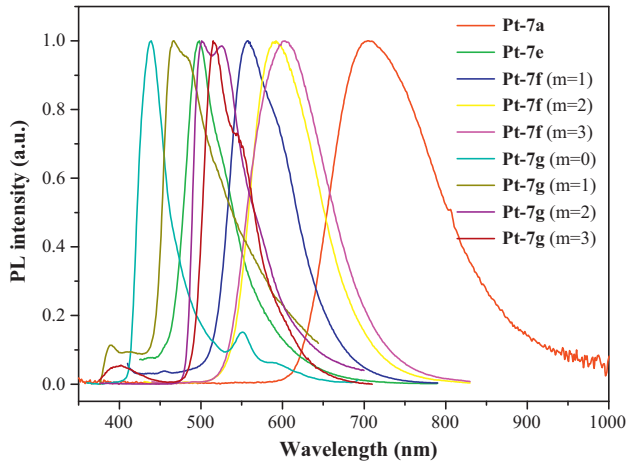

Fig. 8. Fluorescence spectra of polyplatinynes exhibiting a full color spectrum (see Ref. [109,116–118]).

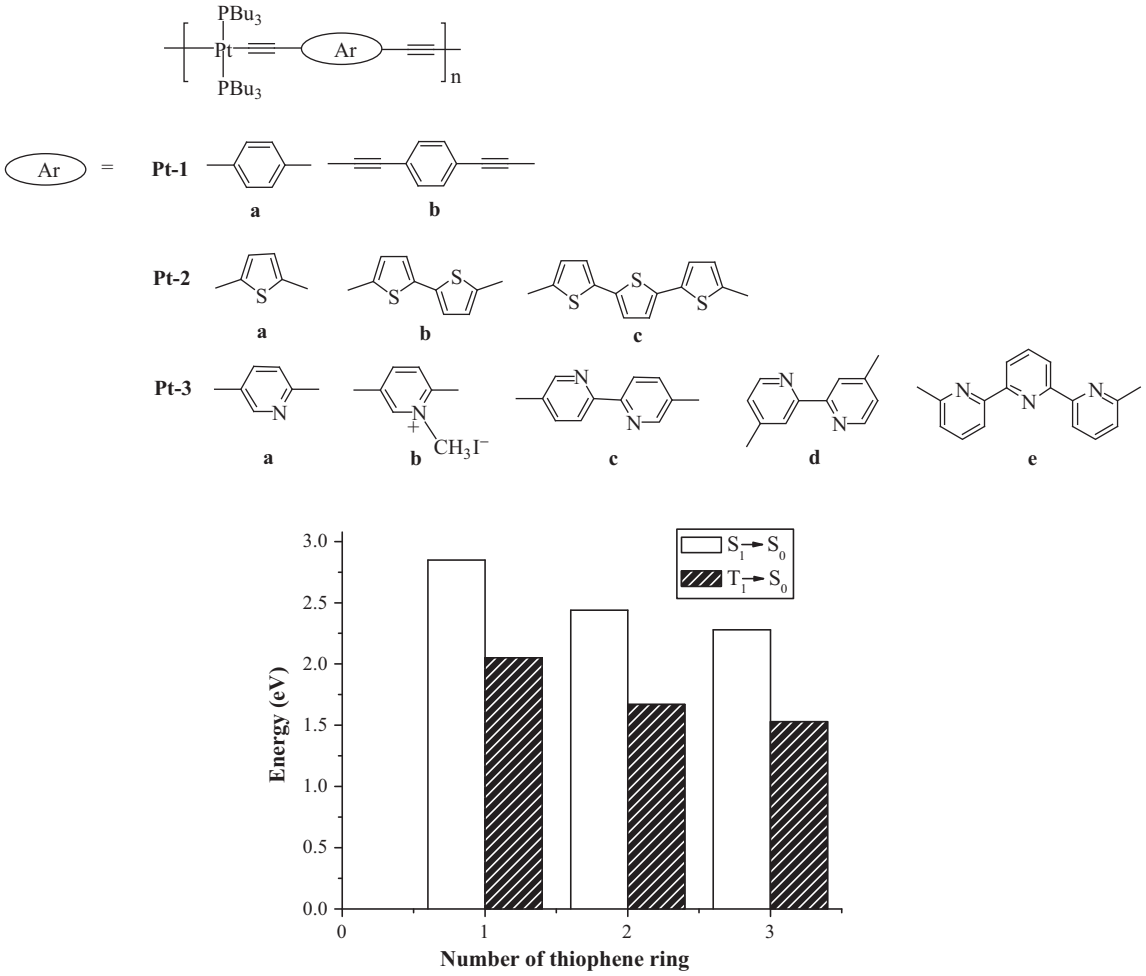

Fig. 9. Energy versus number of thiophene ring dependence of **Pt-2** (see Ref. [92]).

chain to the strongly electron-withdrawing dicyanomethylene group.

As revealed from the absorption features, the polyplatinyne with 3,6-carbazole unit would limit the effective conjugation length of the polymer as compared to the fluorene-based congener. The absorption maximum is blue-shifted in **Pt-6f** (λ_{max} = 344 nm) [102] as compared to **Pt-6a** (λ_{max} = 399 nm) and the phosphorescence wavelength is also tuned from **Pt-6f** (462 nm) to **Pt-6a** (554 nm). The 2,7-substituted carbazole-containing Pt polymer **Pt-6g** has a higher level of conjugation than their 3,6-disubstituted counterpart **Pt-6f** that resulted in luminescent properties similar to the 2,7-fluorene analogue [107]. The E_g of **Pt-6g** was 2.95 eV which is comparable to the 2,7-fluorene-based polymer **Pt-6a** (E_g = 2.96 eV) and is obviously dropped from the polymer bearing the isomeric 3,6-carbazole unit **Pt-6f** (E_g = 3.10 eV). Evidently, the linkage pattern of the bridging moiety in the Pt polymers has a major influence on their UV and PL properties. A relatively high phosphorescence efficiency was found for **Pt-6g** (Φ_{PL} = 2.5%) which is quite unusual for carbazole-containing metalated compounds. Although **Pt-6f** only shows a weak blue fluorescence, an intense greenish yellow light is obtained from an electrophosphorescent PLED based on **Pt-6g** showing a maximum EQE of 1.45%, PE of 1.59 lm W^{-1} and LE of 4.66 cd A^{-1}.

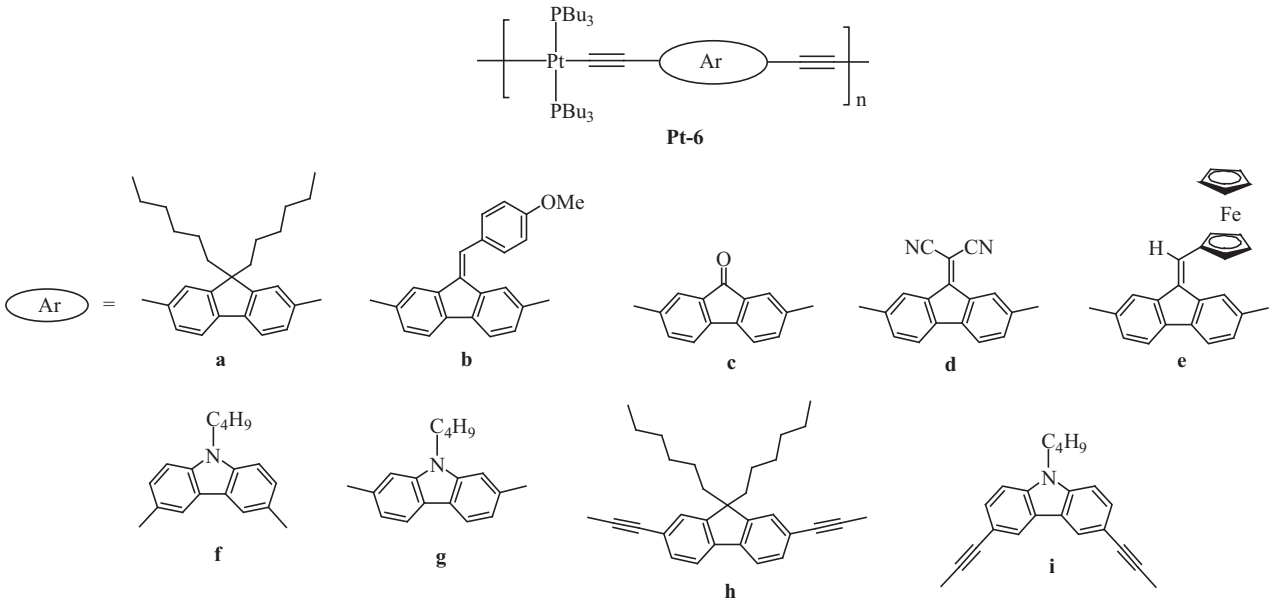

By doubling the acetylenic chain length from **Pt-6a** to **Pt-6h**, a red shift in both the absorption and phosphorescence peaks was noted [108]. The marked bathochromism in the wavelengths is probably attributed to an increased delocalization of π-electrons along the backbone. The triplet energy values are higher for the diethynyl species than for those of the bis(butadiynyl) congeners, giving rise to much larger phosphorescence quantum efficiencies in the former. Extension of the C≡C unit gives rise to a state of lower triplet energy and is accompanied by a decrease in the triplet quantum yield and lifetime. The same observation was also found for the **Pt-6f** and **Pt-6i** pair. Some of these Pt polymers **Pt-6a**, **Pt-6b**, **Pt-6d** and **Pt-6f** exhibit interesting optical-limiting behavior [103]. By comparing the optical limiting responses of **Pt-6a** and **Pt-6f** with their purely organic polyynes, the optical-limiting capability of the organic polyynes can be markedly improved through the insertion of heavy metal ions to the main chains. According to the experimental data and the five-level model for the reverse saturable absorption mechanism, it is the triplet excited-state absorption that contributes to the observed nanosecond optical-limiting process in **Pt-6a** and **Pt-6f**. These results certainly indicate that these platinum polyynes are very valuable optical-limiting materials that should have great potential to excel in the advancement of practical devices.

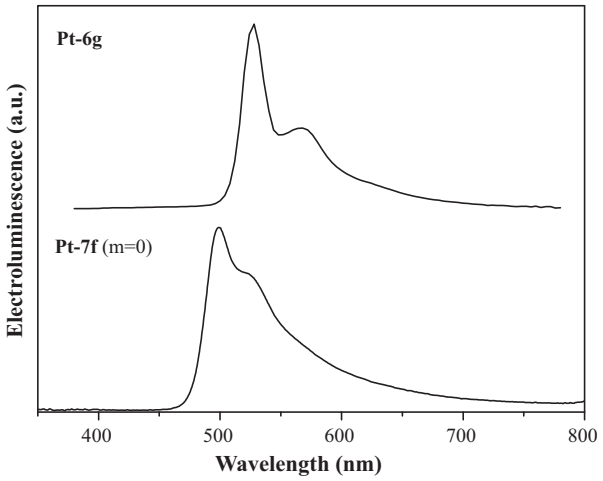

Fig. 10. EL spectra of **Pt-6g** and **Pt-7f** ($m = 0$) doped devices at different doping concentrations (see Ref. [107,118]).

In recent years, the photoconducting properties of conjugated polymers have received increasing attention because of their potential to replace inorganic semiconductors in the development of photovoltaic devices. The D–A structural motif of ligand and incorporation of this unit into the Pt-acetylide chain in **Pt-7** make the resultant materials useful to act as an active layer in solar cell fabrication. Because of the mixed D–A features of the thiazole ring as compared to the thienyl analogue (**Pt-2**), a luminescent bithiazole bridged polyyne **Pt-7e** was made with a low E_g at 2.40 eV [109]. For **Pt-7e**, the absorption peaks show a notable spectral red shift as compared to **Pt-2b**, due to the electron-withdrawing property of the imine nitrogen atom. Moreover, **Pt-7e** can also be used as a green light source in PLED (Fig. 10). For the polymer with a quinoxaline spacer (**Pt-7n**) [110,111], their absorption spectra ($E_g \sim 2.25$ eV) reveal substantial D–A interactions between the Pt center and the conjugated spacer. Detailed studies on the device physics of PLEDs made from **Pt-7n** were described in a seminal paper [31]. Thanks to the push and pull interaction between the electron-donating metal-alkyne and the electron-withdrawing thieno[3,4-*b*]pyrazine unit, a very low band gap was detected for **Pt-7h** to **Pt-7m** ($E_g = 1.47$–2.25 eV) [112–115]. In general, the lifetimes and intensities of phosphorescence are also dramatically reduced with decreasing energy gap.

Recently, Wong et al. prepared a new family of thiophene-based Pt polyynes with strong visible absorption and low E_g induced by the presence of various A groups. Due to the unique D–A features, **Pt-7a** is purple in color with $E_g = 1.85$ eV [116]. A real breakthrough on organometallic photovoltaic cells came out based on this polymer. The bulk heterojunction solar cells consisting of **Pt-7a** and [6,6]-phenyl-C_{61}-butyric acid methyl ester (PCBM) exhibit substantial photovoltaic responses with an average power conversion efficiency (PCE) of 4.1%, even without annealing or the addition of optical spacer layers. A lower E_g contributes to a wide solar spectral coverage in **Pt-7a** as compared to **Pt-2a**. The PCE of the device using **Pt-2a** was only 0.27%, which can be attributed to low coverage of the solar spectrum of **Pt-2a** (with absorption peak at 400 nm). Other polymers featuring D–A motifs were also prepared and in each of these cases, inclusion of various thiophene fragments is likely to further expand the spectral width of absorption appropriate for sunlight harvesting. Most of the optical absorption spectra of this kind of polymers are characterized by two bands. The one at the lower wavelength region (<450 nm) is ascribed to the π–π^* transition. The other lowest-energy absorption features (>450 nm) are

lowered significantly when the metal unit is introduced and these energy bands are due to intramolecular charge transfer (ICT) interaction between the thiophene donor and the different A moieties. The ICT strength increases with the strength of A which would govern the extent of bathochromic shift in the absorption band. The energy gap can be easily fine-tuned by appropriate choice of A. For example, by changing A from 2,1,3-benzothiadiazole (**Pt-7a**) to thieno[3,4-*b*]pyrazines (**Pt-7h** to **Pt-7m**), a gradual red-shift of the ICT absorption band was observed with λ_{max} ranging from 532 to 653 nm (E_g from 1.85 to 1.47 eV). For the polymers bearing central fluorene units (**Pt-7g**) [117], due to the good electron-donating ability of both chromophores, the D–A interaction in this series is weaker and higher E_g values are detected (e.g. E_g = 2.60 eV for **Pt-7g** with the number of thiophene ring, *m*, being 1). Alternatively, the E_g in such series can be significantly lowered by an extended π-electron delocalized system through covalently coupled oligothiophene segment in the organic spacers. The E_g values of **Pt-7g** vary from 2.93 to 2.33 eV as *m* increases. The same phenomenon was observed in other cases with different A linkers such as **Pt-7f**. The facile functionalization of thiophene groups also offers relatively efficient synthetic solutions to address issues concerning solubility and polarity of the polymers. However, the extent of red-shifts induced by *m* is less pronounced and there would be little benefit in extending the π-conjugation by increasing *m* above a certain number. Taking the polymer series **Pt-7f** as an example [118], a linear oligothienyl chain length dependence of E_g can be rationalized from the plot of E_g against reciprocal chain length and a limiting value for E_g is estimated to be ca. 1.96 eV for $m = \infty$.

Efforts were also made to extend the absorption profiles to the NIR region and this requires the development of very low-gap materials. So far, the lowest E_g value was observed for polymers containing thienopyrazine-thiophene (E_g = 1.50 for **Pt-7i** and 1.47 eV for **Pt-7j**) [114,115] and cyclopentadithiophenone-thiophene (E_g = 1.53 eV for **Pt-7p** and 1.44 eV for **Pt-7q**) spacers [119].

In terms of photovoltaic behavior, the solar cell performance of the low-gap polymers depends on their structural motifs significantly. Generally, the larger the *m* value is, the higher the PCE is. In the fluorene-based polyplatinynes (**Pt-7g**), at the same polymer:PCBM blend ratio of 1:5, the PCE increases sharply from *m* = 0 to *m* = 3 in **Pt-7g** and it is remarkable to see that the light-harvesting ability of **Pt-7g** (*m* = 3) can be increased by 8 times relative to (*m* = 0) simply by adding altogether six thienyl rings along the main chain. Moreover, there is a considerable increase in the short-circuit current density (J_{sc}) as *m* increases (Fig. 11). The increase in *m* is also expected to result in an increase of the intrachain mobility because of more extended π-conjugation according to the space charge limited current (SCLC) modeling studies (Fig. 12) [117].

Besides solar cells, functional polyplatinynes reveal potential application in organic field-effect transistors (OFETs), which can be utilized in active-matrix back planes for flexible displays, sensors, and low-cost memory devices [120]. In the proof-of-concept experiments, the semiconducting properties of **Pt-7a** to **Pt-7d** were first demonstrated by measuring their mobilities using an OFET configuration [121]. The OFET capabilities of **Pt-7k**, **Pt-7l** and

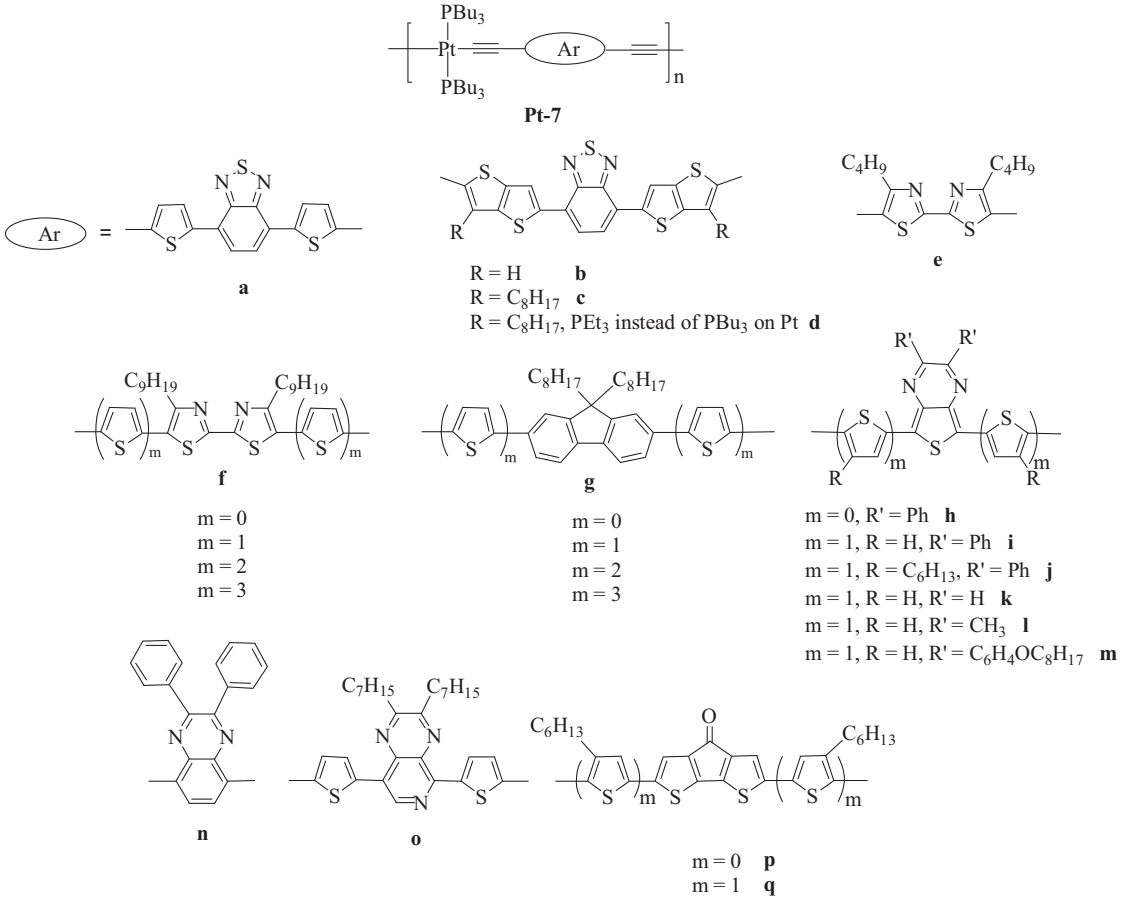

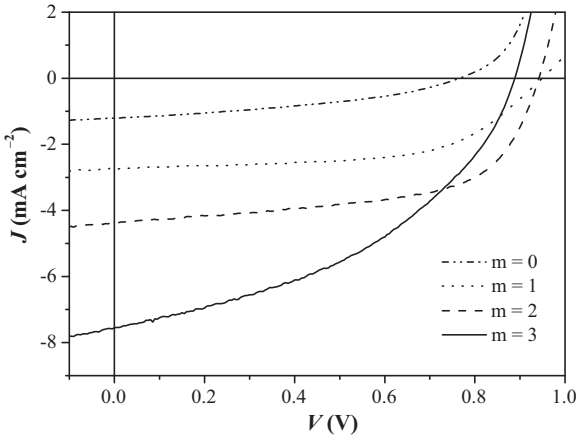

Fig. 11. *J–V* curves of solar cells with **Pt-7g**:PCBM (1:5) active layers under simulated AM1.5 solar irradiation (see Ref. [117]).

Pt-7o were also reported [113]. We observed *p*-channel characteristics in all cases. Compared to **Pt-7a**, the μ_h and on/off ratio significantly improved from 6.1×10^{-5} cm^2 V^{-1} s^{-1} and $\sim 10^2$ to 1.5×10^{-3} cm^2 V^{-1} s^{-1} and $\sim 10^4$ in **Pt-7b**. By using the rigid spacer in **Pt-7d** to enhance the electron coupling between the D and A units, μ_h even improved to 0.01 cm^2 V^{-1} s^{-1} with very high current modulation of >10^6.

6.2. Cyclometalated Pt-based polymer systems

Other than acetylide-based polymers, a new class of Pt-containing conjugated polymers **Pt-8** with decent optoelectronic properties was also reported that is suitable for photovoltaic applications. These polymers contain a Pt(C^N) chromophore chelated with an O^O diketonate ligand in which the Pt is adjacent to the conjugated backbone and connects the aryl groups into a coplanar conformation. In contrast to the polyplatinyne, the platinum atom is peripheral to the conjugated polymer backbone, leading to a greater involvement from the orbitals of Pt in both the ground and excited states of the material [122]. This approach attempts to minimize any potential decrease in effective conjugation length from the poor overlap of Pt and C orbitals, and creates a platform for the study of the influence of a heavy atom on more diffuse excitons. This design also provides flexibility in tuning the absorption profile and energy levels of the materials simply by varying the Pt-ligand chromophore and comonomer. Polymers **Pt-8a** and **Pt-8b** with 2-(2′-thienyl)thiazole-based C^N ligand furnishes a structure analogous to a fused bithiophene system [123]. Both of them exhibit a strong transition at approximately 350 nm, which, given the similarity between this peak and the absorption profile of their Pt complex monomers, is attributed to the direct excitation of the metal complex. Both polymers also show strong transitions at the longer wavelengths, with peaks at 610 and 520 nm for **Pt-8a** and **Pt-8b**, respectively, in solutions (Table 4). These peaks are attributed to excitations delocalized along the conjugated polymer chain. The absorption for **Pt-8b** is significantly red-shifted when compared to those of the platinated polyfluorenes **Pt-8c** and **Pt-8d** [124]. Changing the C^N ligand in the fluorene copolymers from 2-phenylpyridine in **Pt-8c** or **Pt-8d** to 2-(2′-thienyl)thiazole in **Pt-8b** causes the lower energy absorption maximum to shift from 450 to 520 nm. Since Pt complexes containing 2-phenylpyridine and 2-(2′-thienyl)-thiazole have similar absorption spectra, this larger bathochromic shift suggests **Pt-8b** to possess significant D–A character. Therefore, these results show that the optical properties of these Pt-containing polymers can be tuned by modifying either or both of the Pt complex and the comonomer. All of these polymers probed very weak emission with small Stokes shift at room temperature signaling the emission to arise from their singlet excited state. While the nature of the diketonate ligand does not affect the optical properties very much, the spectral positions, shapes and excited lifetimes of **Pt-8c** and **Pt-8d** are very similar.

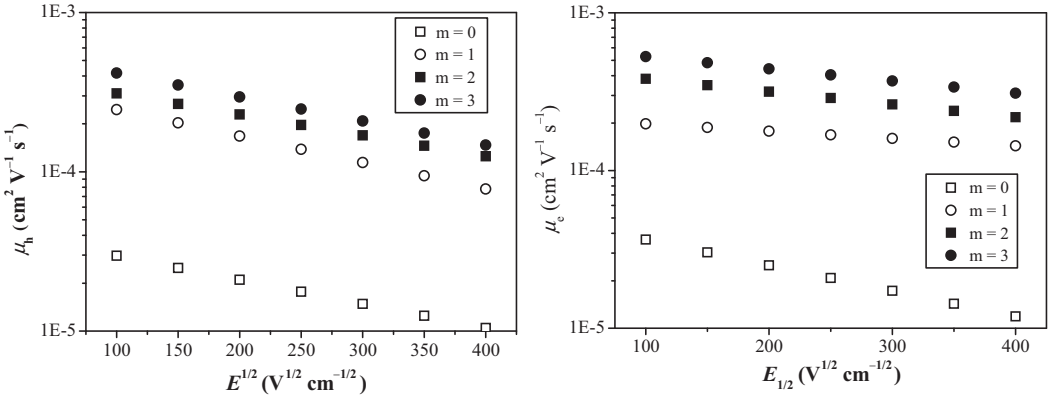

Fig. 12. The comparison between hole (μ_h) (left) and electron (μ_e) (right) mobilities in **Pt-7g**:PCBM blends obtained by the SCLC modeling (see Ref. [117]).

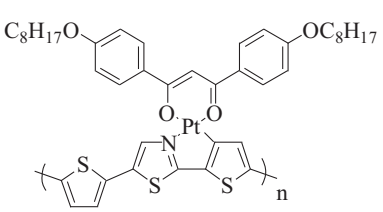

Pt-8a

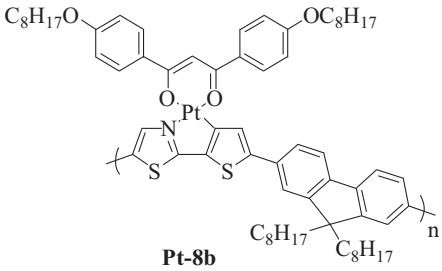

Pt-8b

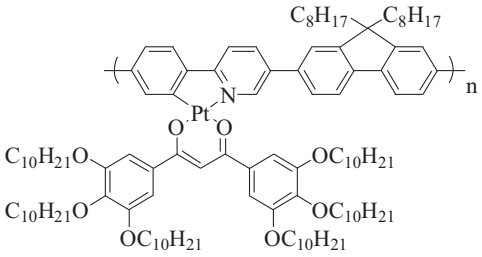

Pt-8c

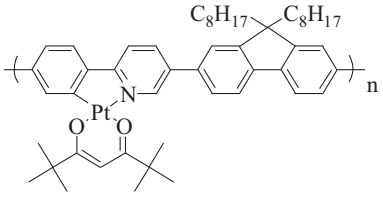

Pt-8d

6.3. Mixed-metal systems

Synthesis of metalloporphyrin-containing Pt polymers **Pt-9** was reported by Harvey and his co-workers. The absence of conjugation throughout the polymer chain in **Pt-9a** and **Pt-9b** is due to the presence of two methyl groups at the β-positions that precludes rotation of the C_6H_4 group for appropriate π-overlaps [125]. The absence or weakly presence of conjugation is readily demonstrated from the amplitude of the red-shifting of the porphyrin Soret and Q bands upon the increase in molecular dimension. Because of the non-conjugated or partially conjugated behavior of these polymers, the chromophores in these systems are almost distinct (but not independent), notably *trans*-$C_6H_4C{\equiv}C{-}PtL_2{-}C{\equiv}CC_6H_4$ and metalloporphyrin. The fully conjugated Pt–porphyrin systems were also recently investigated as **Pt-9c** and **Pt-9d** [126]. The use of long soluble chains such as $OC_{16}H_{33}$ has helped to render the as-prepared polymers soluble. The direct bonding between the metalloporphyrins and the Pt makes the systems extensively conjugated. The electronic communication between the two metalloporphyrin units was confirmed by spectroelectrochemistry where intervalence bands were detected in the electronic spectra in the NIR region.

A prominent class of phosphorescent oligometallaynes (**Pt-10** and **Pt-11**) of dual metal centers (Ir and Pt) was recently designed by Zhou et al. [127]. **Pt-11** with fluorene moiety as the cyclometalating ligand exhibits a red-shift in both absorption and emission features as compared to **Pt-10**. Upon light irradiation, **Pt-10** and **Pt-11** both produce intense yellow/orange phosphorescence. The enhanced conjugation effect of the ppy-type ligands chelated with an Ir center after copolymerization would lead to bathochromic behavior for the emission maxima of **Pt-10** and **Pt-11**. A maximum brightness of 3356 cd m^{-2} (or 2708 cd m^{-2}), EQE of 0.50% (or 0.67%), LE of 1.59 cd A^{-1} (or 1.55 cd A^{-1}) and PE of 0.60 lm W^{-1} (or 0.55 lm W^{-1}) for the yellow (or orange) phosphorescent PHOLEDs were detected for **Pt-10** (or **Pt-11**).

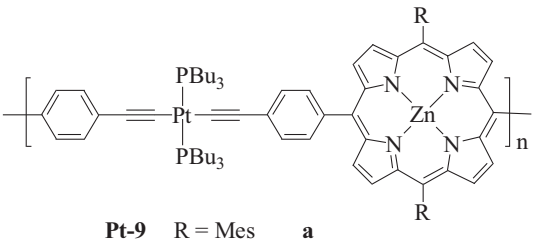

Pt-9 R = Mes **a**
n-C_5H_{11} **b**

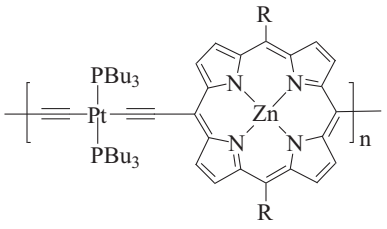

R = Mes **c**

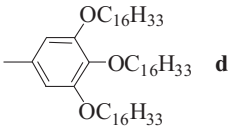

d

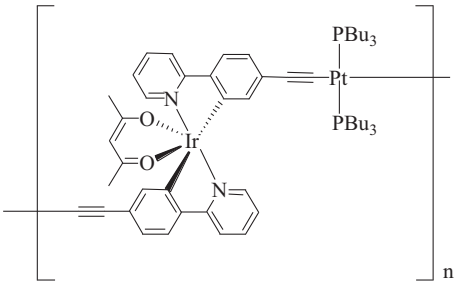

Pt-10

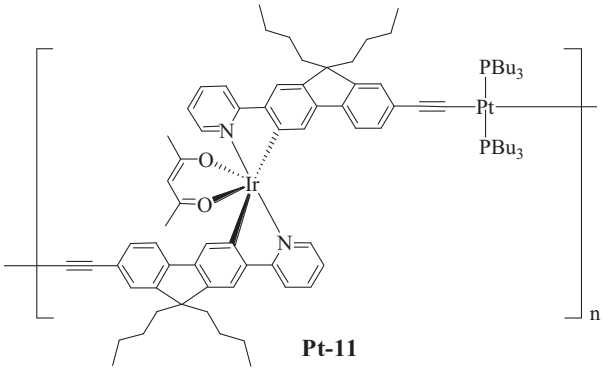

Pt-11

7. Conclusion and future perspectives

Polymeric semiconductors are attracting much current attention in the scientific community and one key focus is shifted toward utilizing them in energy research in the recent years. The transformations of light into electricity and electricity into light represent two complementary but important topics that are highly relevant to the solution of the worldwide energy problem. Inorganic chemistry is particularly vital to such development. Coordination and organometallic compounds have been widely investigated in these energy-generating and energy-saving applications. These energy conversion materials can play key roles in the safe and efficient production, transformation and utilization of the two energy forms. In the past decade, impressive progress has been made in this research frontier and this article provides a detailed survey of the syntheses, photophysics and optoelectronic/photonic applications of metallopolymers. The chemical and physical properties of these polymers can be fine-tuned simply by varying their molecular structures via chemical modifications of their metal and ligand chromophores to develop the best materials to fit a particular function. New emerging applications can also be realized with polymers possessing multifunctional utilities. From a survey of literature data, metallopolymers based on Ru(II) ions are generally suitable for light-harvesting applications while those with Ir(III) cyclometalates are better for many light-emitting purposes and their PLED efficiencies are often higher than the polymers derived from the Zn(II)-terpyridine chromophores. Impressively, polymetallaynes of Pt(II) have good potentials to serve as active materials for both applications depending on their optical properties. We feel that the novelty in the coming years will be on the mixed-metal systems and the number of combinations is basically countless. For instance, the heterometallic polymers would be good precursors toward the generation of new types of metal alloy nanoparticles and ceramics for magnetic applications [128,129]. The area will continue to expand with the discovery of increasingly exquisite methods of polymer synthesis and rapid scientific advances at the key interfaces of supramolecular chemistry, physics and biology. Molecular control of the materials properties and rational design of new generation materials through innovative chemical synthesis will certainly lead to a prosperous future of this field for many years to come.

Acknowledgements

W.-Y. Wong thanks the Croucher Foundation for the Croucher Senior Research Fellowship, Hong Kong Baptist University (FRG2/09-10/091), the Hong Kong Research Grants Council (HKBU202410) and a grant from Areas of Excellence Scheme, University Grants Committee, Hong Kong (Project No. AoE/P-03/08). Technical support from Miss Lai-Fan Lai is also gratefully acknowledged.

References

[1] E. Holder, B.M.W. Langeveld, U.S. Schubert, Adv. Mater. 17 (2005) 1109.
[2] C.J. Brabec, N.S. Sariciftci, J.C. Hummelen, Adv. Funct. Mater. 11 (2001) 15.
[3] S. Günes, H. Neugebauer, N.S. Sariciftci, Chem. Rev. 107 (2007) 1324.
[4] J. Liu, J.W.Y. Lam, B.Z. Tang, Chem. Rev. 109 (2009) 5799.
[5] G.R. Whittell, I. Manners, Adv. Mater. 19 (2007) 3439.
[6] A.S. Abd-El-Aziz, P.O. Shipman, B.N. Boden, W.S. McNeil, Prog. Polym. Sci. 35 (2010) 714.
[7] B.J. Holliday, T.M. Swager, Chem. Commun. (2005) 23.
[8] W.-Y. Wong, C.-L. Ho, Acc. Chem. Res. 23 (2010) 1246.
[9] W.-Y. Wong, Macromol. Chem. Phys. 209 (2008) 14.
[10] T.J. Meyer, Acc. Chem. Res. 22 (1989) 163.
[11] S.C. Yu, S.J. Hou, W.K. Chan, Macromolecules 33 (2000) 3259.
[12] R. Grigg, J.M. Holmes, S.K. Jones, W. Norbert, J. Chem. Soc. Chem. Commun. (1994) 185.
[13] J.K. Lee, D. Yoo, M.F. Rubner, Chem. Mater. 9 (1997) 1710.
[14] A. Kraft, A.C. Grimsdale, A.B. Holmes, Angew. Chem. Int. Ed. Engl. 37 (1998) 402.
[15] K.A. Walters, K.D. Ley, K.S. Schanze, Chem. Commun. (1998) 1115.
[16] K.D. Ley, Y.T. Li, J.V. Johnson, D.H. Powell, K.S. Schanze, Chem. Commun. (1999) 1749.
[17] K.D. Ley, C.E. Whittle, M.D. Bartberger, K.S. Schanze, J. Am. Chem. Soc. 119 (1997) 3423.
[18] J.L. Segura, N. Martin, J. Mater. Chem. 10 (2000) 2403.

[19] A. Juris, V. Balzani, F. Barigelletti, S. Campagna, P. Belser, A. von Zelewsky, Coord. Chem. Rev. 84 (1988) 85.
[20] E. Yashima, T. Matsushima, Y. Okamoto, J. Am. Chem. Soc. 119 (1997) 6345.
[21] T. Masuda, K.I. Hasegawa, T. Higashim, Macromolecules 7 (1974) 728.
[22] W. Scherman, G. Wegner, Makromol. Chem. 175 (1974) 667.
[23] E.T. Kang, P. Ehrlich, A. Bhatt, W. Anderson, Macromolecules 17 (1984) 1020.
[24] B.Z. Tang, N. Kotera, Macromolecules 22 (1989) 4388.
[25] T. Masuda, T. Hamano, K. Tsuchihara, T. Higashimura, Macromolecules 23 (1990) 1374.
[26] Z. Xu, M. Kahr, K.L. Walker, C.L. Wilkins, J.S. Moore, J. Am. Chem. Soc. 116 (1994) 4537.
[27] Y. Kishimoto, P. Eckerle, T. Miyatake, T. Ikariya, R. Noyori, J. Am. Chem. Soc. 116 (1994) 12131.
[28] H.-J. Lee, Y.-S. Gal, W.-C. Lee, J.-M. Oh, S.-H. Jin, S.-K. Choi, Macromolecules 28 (1995) 1208.
[29] H. Nishide, T. Kaneko, T. Nii, K. Katoh, E. Tsuchida, P.M. Lahti, J. Am. Chem. Soc. 118 (1996) 9695.
[30] M.A. Baldo, D.F. O'Brien, Y. You, A. Shoustikov, S. Sibley, M.E. Thompson, S.R. Forrest, Nature 395 (1998) 151.
[31] J.S. Wilson, A.S. Dhoot, A.J.A.B. Seeley, M.S. Khan, A. Kohler, R.H. Friend, Nature 413 (2001) 828.
[32] A. Winter, C. Friebe, M. Chiper, M.D. Hager, U.S. Schubert, J. Polym. Sci. A: Polym. Chem. 47 (2009) 4083.
[33] K. Morisige, Anal. Chim. Acta 22 (1974) 295.
[34] C.-C. Kwok, S.-C. Yu, I.H.T. Sham, C.-M. Che, Chem. Commun. (2004) 2758.
[35] Q. Peng, M. Xie, Y. Huang, Z. Lu, Y. Cao, Macromol. Chem. Phys. 206 (2005) 2373.
[36] E.C. Constable, Macromol. Symp. 98 (1995) 503.
[37] R. Dobrawa, F. Würthner, Chem. Commun. (2002) 1878.
[38] S.-Y. Yu, C.-C. Kwok, W.-K. Chan, C.-M. Che, Adv. Mater. 15 (2003) 1643.
[39] F. Schlütter, A. Wild, A. Winter, M.D. Hager, A. Baumgaertel, C. Friebe, U.S. Schubert, Macromolecules 43 (2010) 2759.
[40] J. Roncali, Chem. Rev. 97 (1997) 173.
[41] M. Shahid, R.A. Shahid, E. Klemm, S. Sensfuss, Macromolecules 39 (2006) 7844.
[42] W.-C. Wu, W.-Y. Lee, C.-L. Pai, W.-C. Chen, C.-S. Tuan, J.-L. Lin, J. Polym. Sci. B: Polym. Phys. 45 (2006) 67.
[43] Y.-Y. Chen, H.-C. Lin, J. Polym. Sci. A: Polym. Chem. 45 (2007) 3243.
[44] A. Meyers, C. South, M. Weck, Chem. Commun. (2004) 1176.
[45] K. Kalyanasundaram, Coord. Chem. Rev. 46 (1982) 159.
[46] T. Yamamoto, Y. Yoneda, T. Maruyama, J. Chem. Soc. Chem. Commun. (1992) 1652.
[47] N. Hayashida, T. Yamamoto, Bull. Chem. Soc. Jpn. 72 (1999) 1153.
[48] S.C. Yu, X. Gong, W.K. Chan, Macromolecules 31 (1998) 5639.
[49] Z. Peng, L. Yu, J. Am. Chem. Soc. 118 (1996) 3777.
[50] Q. Wang, L. Yu, J. Am. Chem. Soc. 122 (2000) 11806.
[51] Z. Peng, A.R. Gharavi, L. Yu, J. Am. Chem. Soc. 119 (1997) 4622.
[52] P.K. Ng, X. Gong, S.H. Chan, L.S.M. Lam, W.K. Chan, Chem. Eur. J. 7 (2001) 4358.
[53] K.A. Walters, L. Trouillet, S. Guillerez, K.S. Schanze, Inorg. Chem. 39 (2000) 5496.
[54] S.C. Yu, S. Hou, W.K. Chan, Macromolecules 32 (1999) 5251.
[55] K.Y.K. Man, H.L. Wong, W.K. Chan, Langmuir 22 (2006) 3368.
[56] W.Y. Ng, X. Gong, W.K. Chan, Chem. Mater. 11 (1999) 1165.
[57] C.T. Wong, W.K. Chen, Adv. Mater. 11 (1999) 455.
[58] Y. Liu, S. Jiang, K.S. Schanze, Chem. Commun. (2003) 650.
[59] K.W. Cheng, C.S.C. Mak, W.K. Chan, A.M.C. Ng, A.B. Djurišic, J. Polym. Sci. A: Polym. Chem. 46 (2008) 1305.
[60] K. Peter, M. Thelakkat, Macromolecules 36 (2003) 1779.
[61] Y.-S. Cho, H.-K. Lee, J.-S. Lee, Macromol. Chem. Phys. 203 (2002) 2495.
[62] V. Marin, E. Jolder, M.A.R. Meier, R. Hoogenboom, U.S. Schubert, Macromol. Rapid Commun. 25 (2004) 793.
[63] V. Marin, E. Jolder, R. Hoogenboom, U.S. Schubert, J. Polym. Sci. A: Polym. Chem. 42 (2004) 4153.
[64] J. Langecker, M. Rehahn, Macromol. Chem. Phys. 209 (2008) 258.
[65] T. Ito, S. Suzuki, J. Kido, Polym. Adv. Technol. 16 (2005) 480.
[66] H. Zhen, C. Jiang, W. Yang, J. Jiang, F. Juang, Y. Cao, Chem. Eur. J. 11 (2005) 5007.
[67] W.-S. Huang, Y.-H. Wu, H.-C. Lin, J.T. Lin, Polym. Chem. 1 (2010) 494.
[68] H. Zhen, J. Luo, W. Yang, Q. Chen, L. Ying, Z. Jianhua, H. Wu, Y. Cao, J. Mater. Chem. 17 (2007) 2824.
[69] H. Zhen, W. Xu, W. Yang, Q. Chen, Y. Xu, J. Jiang, J. Peng, Y. Cao, Macromol. Rapid Commun. 27 (2006) 2095.
[70] Q. Chem, N. Liu, L. Ying, W. Yang, H. Wu, W. Hu, Y. Cao, Polymer 50 (2009) 1430.
[71] S.-J. Liu, Q. Zhao, R.-F. Chen, Y. Deng, Q.-L. Fan, F.-Y. Li, L.-H. Wnag, C.-H. Hunag, W. Huang, Chem. Eur. J. 12 (2006) 4351.
[72] Y. Deng, S.-J. Liu, Q.-L. Fan, R. Zhu, K.-Y. Pu, L.-H. Yumen, L.-H. Wang, W. Huang, Synth. Met. 157 (2007) 813.
[73] S.-J. Liu, Q. Zhao, Y. Deng, Y.-J. Xia, J. Lin, Q.-L. Fan, L.-H. Wang, W. Huang, J. Phys. Chem. C 111 (2007) 1166.
[74] K. Zhang, Z. Chen, C. Yang, S. Gong, J. Qin, Y. Cao, Macromol. Rapid Commun. 27 (2006) 1926.
[75] M.-J. Park, J. Kwak, J. Lee, I.H. Jung, H. Kong, C. Lee, D.-H. Hwang, H.-K. Shim, Macromolecules 43 (2010) 1379.
[76] K. Zhang, Z. Chen, C. Yang, Y. Zou, S. Gong, Y. Tao, J. Qin, Y. Cao, J. Mater. Chem. 18 (2008) 3366.
[77] W. Yang, H.Y. Zhen, C.Y. Jiang, L.J. Su, J.X. Jiang, H.H. Shi, Y. Cao, Synth. Met. 153 (2005) 189.
[78] R. Guan, Y. Zu, L. Ying, W. Yang, H. Wu, Q. Chen, Y. Cao, J. Mater. Chem. 19 (2009) 531.
[79] X. Chen, J.-L. Liao, Y. Liang, M.O. Ahmed, H.-E. Tseng, S.A. Chen, J. Am. Chem. Soc. 125 (2003) 636.
[80] B. Du, L. Wang, H. Wu, W. Yang, Y. Zhang, R. Liu, M. Sun, J. Peng, Y. Cao, Chem. Eur. J. 13 (2007) 7432.
[81] Z. Ma, J. Ding, B. Zhang, C. Mei, Y. Cheng, Z. Xie, L. Wang, X. Jing, F. Wang, Adv. Funct. Mater. 20 (2010) 138.
[82] C. Mei, J. Ding, B. Yao, Y. Cheng, Z. Xie, Y. Geng, L. Wang, J. Polym. Sci. A: Polym. Chem. 45 (2007) 1746.
[83] J. Jiang, Y. Xu, W. Yang, R. Guan, Z. Lin, H. Zhen, Y. Cao, Adv. Mater. 18 (2006) 1769.
[84] X.-H. Yang, F.-I. Wu, D. Neher, C.-H. Chein, C.-F. Shu, Chem. Mater. 20 (2008) 1629.
[85] X.-Y. Wang, A. Kimyouok, M. Weck, Chem. Commun. (2006) 3933.
[86] D.A. Poulsen, B.J. Kim, B. Ma, C.S. Zonte, J.M.J. Fréchet, Adv. Mater. 22 (2010) 77.
[87] Y. Fujikura, K. Sonogashira, N. Hagihara, Chem. Lett. (1975) 1067.
[88] S. Takahashi, M. Kariya, T. Yatake, K. Sonogashira, N. Hagihara, Macromolecules 11 (1978) 1063.
[89] K. Sonogashira, S. Takahashi, N. Hagihara, Macromolecules 10 (1977) 879.
[90] R.D. Markwell, I.S. Butler, A.K. Kakkar, M.S. Khan, Z.H. Al-Zakwani, J. Lewis, Organometallics 15 (1996) 2331.
[91] J. Lewis, M.S. Khan, B.F.G. Johnson, T.B. Marder, H.B. Fyfe, F. Wittmann, R.H. Friend, A.E. Dray, J. Organomet. Chem. 425 (1992) 165.
[92] N. Chawdhury, A. Köhler, R.H. Friend, W.-Y. Wong, J. Lewis, M. Younus, P.R. Raithby, T.C. Corcoran, M.R.A. Al-Mandhary, M.S. Khan, J. Chem. Phys. 110 (1999) 4963.
[93] K.A. Bunten, A.K. Kakkar, J. Mater. Chem. 5 (1995) 2041.
[94] M.S. Khan, M.R.A. Al-Mandhary, M.K. Al-Suti, A.K. Hisahm, P.R. Raithby, B. Ahrens, M.F. Mahon, L. Male, E.A. Marseglia, E. Tedesco, R.H. Friend, A. Köhler, N. Feeder, S.J. Teat, J. Chem. Soc. Dalton Trans. (2002) 1358.
[95] N. Chawdhury, A. Köhler, R.H. Friend, M. Younus, N.J. Long, P.R. Raithby, J. Lewis, Macromolecules 31 (1998) 722.
[96] W.-Y. Wong, C.-K. Wong, G.-L. Lu, K.-W. Cheah, J.-X. Shi, Z. Lin, J. Chem. Soc. Dalton Trans. (2002) 4587.
[97] W.-Y. Wong, C.-K. Wong, G.-L. Lu, A.W.-M. Lee, K.-W. Cheah, J.-X. Shi, Macromolecules 36 (2003) 983.
[98] W.-Y. Wong, S.-Y. Poon, J.-X. Shi, K.-W. Cheah, J. Polym. Sci. A: Polym. Chem. 44 (2006) 4804.
[99] W.-Y. Wong, S.-Y. Poon, J.-X. Shi, K.-W. Cheah, J. Inorg. Organomet. Polym. Mater. 17 (2007) 189.
[100] W.-Y. Wong, S.-Y. Poon, A.W.-M. Lee, J.-X. Shi, K.-W. Cheah, Chem. Commun. (2004) 2420.
[101] S.-Y. Poon, W.-Y. Wong, K.-W. Cheah, J.-X. Shi, Chem. Eur. J. 12 (2006) 2550.
[102] W.-Y. Wong, G.-L. Lu, K.-H. Choi, J.-X. Shi, Macromolecules 25 (2002) 3506.
[103] G.-J. Zhou, W.-Y. Wong, D. Cui, C. Ye, Chem. Mater. 17 (2005) 5209.
[104] J. Lewis, P.R. Raithby, W.-Y. Wong, J. Organomet. Chem. 556 (1998) 219.
[105] W.-Y. Wong, K.-H. Choi, G.-L. Lu, J.-X. Shi, Macromol. Rapid Commun. 22 (2001) 461.
[106] W.-Y. Wong, W.-K. Wong, P.R. Raithby, J. Chem. Soc. Dalton Trans. (1998) 2761.
[107] C.-L. Ho, C.-H. Chui, W.-Y. Wong, S.M. Aly, D. Fortin, P.D. Harvey, B. Yao, Z. Xie, L. Wang, Macromol. Chem. Phys. 270 (2009) 1786.
[108] L. Liu, W.-Y. Wong, S.-Y. Poon, J.-X. Shi, K.-W. Cheah, Z. Lin, Chem. Mater. 18 (2006) 1369.
[109] W.-Y. Wong, G.-J. Zhou, Z. He, K.-Y. Cheung, A.M.-C. Ng, A.B. Djurišić, W.-K. Chan, Macromol. Chem. Phys. 209 (2008) 1319.
[110] M.S. Khan, M.K. Al-Suti, M.R.A. Al-Mandhary, B. Ahrens, J.K. Bjernemose, M.F. Mahon, L. Male, P.R. Raithby, R.H. Friend, A. Köhler, J.S. Wilson, Dalton Trans. (2003) 65.
[111] J.S. Wilson, A. Köhler, R.H. Friend, M.K. Al-Suti, M.R.A. Al-Mandhary, M.S. Khan, P.R. Raithby, J. Chem. Phys. 113 (2000) 7627.
[112] M. Younus, A. Köhler, S. Cron, N. Chawdhury, M.R.A. Al-Mandhary, M.S. Khan, J. Lewis, N.J. Long, R.H. Friend, P.R. Raithby, Angew. Chem. Int. Ed. 37 (1998) 3036.
[113] P.-T. Wu, T. Bull, F.S. Kim, C.K. Luscombe, S.A. Jenekhe, Macromolecules 42 (2009) 671.
[114] X.-Z. Wang, C.-L. Ho, L. Yan, X. Chen, X. Chen, K.-Y. Cheung, W.-Y. Wong, J. Inorg. Organomet. Polym. Mater. 20 (2010) 478.
[115] X.-Z. Wang, W.-Y. Wong, K.-Y. Cheung, M.-K. Fung, A.B. Djurišić, W.-K. Chan, Dalton Trans. (2008) 5484.
[116] W.-Y. Wong, X.-Z. Wang, Z. He, A.B. Djurišić, C.-T. Yip, K.-Y. Cheung, H. Wang, C.S.-K. Mak, W.-K. Chan, Nat. Mater. 6 (2007) 521.
[117] L. Li, C.-L. Ho, W.-Y. Wong, K.-Y. Cheung, M.-K. Fung, W.-T. Lam, A.B. Djurisic, W.-K. Chan, Adv. Funct. Mater. 18 (2008) 2824.
[118] W.-Y. Wong, X.-Z. Wang, Z. He, K.-K. Chan, A.B. Djurišić, K.-Y. Cheung, C.-T. Yip, A.M.-C. Ng, Y.Y. Xi, C.S.-K. Mak, W.-K. Chan, J. Am. Chem. Soc. 129 (2007) 14372.
[119] X.-Z. Wang, Q. Wang, L. Yan, W.-Y. Wong, K.-Y. Cheung, A. Ng, A.B. Djurišić, W.-K. Chan, Macromol. Rapid Commun. 31 (2010) 861.
[120] G. Horowitz, Adv. Mater. 10 (1998) 365.
[121] N.S. Baek, S.K. Hau, H.-L. Yip, O. Acton, K.-S. Chen, A.K.-Y. Jen, Chem. Mater. 20 (2008) 5734.

[122] J. Brooks, Y. Babayan, S. Lamansky, P.I. Djurovich, I. Tsyba, R. Bau, M.E. Thompson, Inorg. Chem. 41 (2002) 3055.
[123] T.A. Clem, D.F.J. Kavulak, E.J. Westling, J.M.J. Fréchet, Chem. Mater. 22 (2010) 1977.
[124] S.W. Thomas III, S. Yagi, T.M. Swager, J. Mater. Chem. 15 (2005) 2829.
[125] L. Liu, D. Fortin, P.D. Harvey, Inorg. Chem. 48 (2009) 5891.
[126] F.-L. Jiang, D. Fortin, P.D. Harvey, Inorg. Chem. 49 (2010) 2614.
[127] G.-J. Zhou, Y. He, B. Yao, J. Dang, W.-Y. Wong, Z. Xie, X. Zhao, L. Wang, Chem. Asian J. 5 (2010) 2405.
[128] K. Liu, S.B. Clendenning, L. Friebe, W.Y. Chan, X.B. Zhu, M.R. Freeman, G.C. Yang, C.M. Yip, D. Grozea, Z.-H. Lu, I. Manners, Chem. Mater. 18 (2006) 2591.
[129] K. Liu, C.-L. Ho, S. Aouba, Y.-Q. Zhao, Z.-H. Lu, S. Petrov, N. Coombs, P. Dube, H.E. Ruda, W.-Y. Wong, I. Manners, Angew. Chem. Int. Ed. 47 (2008) 1255.